Characterization, Modeling of Piezoelectric Pressure Transducer for Facilitation of Field Calibration

Zahra Pakdel

Thesis submitted to the Faculty of the
Virginia Polytechnic Institute and State University
in partial fulfillment of the requirements for the degree of

MASTER OF SCIENCE
in
Electrical Computer Engineering
APPROVED:

Pushkin Kachroo
Douglas K. Lindner
Lynn A. Abbott

May 21, 2007 Blacksburg, Virginia

Keywords: Charge Amplifier, Electromechanical Sensor, Piezoelectric Effect

Characterization, Modeling of Piezoelectric Pressure Transducer for Facilitation of Field Calibration

Zahra Pakdel

ABSTRACT

Currently in the marketplace, one of the important goals is to improve quality, and reliability. There is great interest in the engineering community to develop a field calibration technique concerning piezoelectric pressure sensor to reduce cost and improve reliability.

This paper summarizes the algorithm used to characterize and develop a model for a piezoelectric pressure transducer. The basic concept of the method is to excite the sensor using an electric force to capture the signature characteristic of the pressure transducer.

This document presents the frequency curve fitted model based on the high frequency excitation of the piezoelectric pressure transducer. It also presents the time domain model of the sensor. The time domain response of the frequency curve fitted model obtained in parallel with the frequency response of the time domain model and the comparison results are discussed. Moreover, the relation between model parameters and sensitivity extensively is investigated.

In order to detect damage and monitor the condition of the sensor on line the resonance frequency comparison method is presented. The relationship between sensitivity and the resonance frequency characteristic of the sensor extensively is investigated. The method of resonance monitoring greatly reduces the cost of hardware.

This work concludes with a software implementation of the signature comparison of the sensor based on a study of the experimental data. The software would be implemented in the control system.

DEDICATIONS

This thesis is dedicated to my father, Mohammad Ali Pakdel (1943-2006). My dad's integrity, love, and compassion for all people left an indelible impression on my life. I will be eternally grateful for his example. Thanks for encouraging me to continue my education.

ACKNOWLEDGMENTS

I would like to thank Dr. Pushkin Kachroo, my advisor, for the many productive discussions. Also, I thank the other two members of my advisory Committee.

Special thanks are extended to two people, without whom I most likely would not have returned to school. First, I thank my husband, Farzad Dadras, for always respecting my decisions and sharing my failures and success with equal eagerness. I thank my precious treasure, Niyousha Dadras, you bring me more joy than I could have ever hoped for! Being your mom is my greatest reward.

And most of all, I thank my mother, sister, and brothers for their unconditional love and support. For all the times you stood by me through my moments of distress, I thank you.

TABLE OF CONTENTS

Page

LIST OF FIGURES

Figure **Page**

CHAPTER I

INTRODUCTION

Currently in the marketplace the goal is to improve quality, reliability and lower cost. There is a great interest in the engineering community to develop a field calibration technique concerning piezoelectric pressure sensors to reduce cost and improve reliability.

Most of the laboratory calibrations are performed by applying mechanical excitation to the pressure transducer while measuring electrical output from the sensor. This work is an experimental study of modeling and characterization of a pressure transducer to apply on line field calibration.

The transducer will send distorted signals and will lead to false information if it has a small fracture in the piezoelectric crystal or in its structure. Moreover, the pressure sensors are usually the most delicate part in the structural system, and their performance can degrade over time. It will be cost effective to detect the degradation in order to identify replacement time.

1.1 Background

One of the major applications of piezoelectricity is in transducers. A transducer is any device that converts one type of energy to another. Pressure sensors are a type of transducer. A pressure sensor generates a signal related to the pressure imposed. Typically, such a signal is electrical. Pressure sensors are often fabricated using thin membranes that flex under pressure. There are many technologies in making pressure sensors. One of the first types of transducers was the microphone, developed in the late 1800s by Thomas Edison. The microphones allow sound waves to vibrate a sensitive cone, which will then be converted to electrical signal. The speaker, which is another type of transducer, takes the electrical signal and converts back to sound.

The amount of voltage produce by a piezoelectric element under pressure is very small. A unique method was developed to increase the amount of voltage produce for a defined amount of applied pressure.

The piezoelectric elements connect together back to back, and they deform in opposite directions under applied voltage. This causes a twisting or bending motion. These elements can be connecting in series or parallel, depending on their application. In parallel connection, one lead goes to the outer electrodes of both elements, and the second lead connects to the inner-facing electrodes. In a series connection, connecting leads attach to the two outer electrodes of the elements, and the two facing inner electrodes are not connected. In order to maximize efficiency and produce maximum

voltage for a given amount of pressure, it is crucial that the piezoelectric element are mounted correctly, and force be applied at the proper point on its surface (Cady 1964).

Piezoelectric pressure sensors are generally designed for dynamic measurements of compression, combustion, explosion, pulsation, cavitations, blast, pneumatic, hydraulic, fluid and other such pressures. They are well suited to measure rapidly changing pressure fluctuations over a wide amplitude and frequency range.

Piezoelectric pressure sensors used in this research contain a diaphragm that is supported by a rigid column of quartz. They have the unique capability to measure low acoustic pressure changes under high static loading as might be involved with fluid borne noise measurements in hydraulic systems. The static components of the signal are eliminated from the sensor output due to the discharge time constant of the sensor.
The electrical output signal from the piezoelectric transducer in all the cases must be amplified before it is used for its intended purpose. When connecting piezoelectric device into a circuit, there are few points that need to consider. The piezoelectric devices have very high impedance.

There are other type of piezoelectric transducer which are widely use by industry and military. One of these devices is piezoelectric shear accelerometer, which is used to accurately measure the vibration of various mechanical objects on vibrations applied to the base of the accelerometer cause production of shear stress in the walls of the cylindrical piezoelectric element. The voltage is proportional to the stresses produced. An oscilloscope can then amplify the results.

Another type of piezoelectric transducer is an underwater sound transducer that detects and analyzes underwater sound waves and pressures. This unit is constructed from a stack

of ammonium dihydrogen phosphate crystal plate. The ends of the plate couple to the water via a rubber housing and oil that surrounds the stack.

A Piezoelectric spark pump is capable of generating voltage as high as 20,000 volts. It consists of two piezoelectric ceramic cylinders placed end to end. When pressure is applied to one end of the cylinder, a voltage will develop at their electrodes. One application of the generator is for internal combustion engine ignition systems.

1.2 Literature Review

A completely broken sensor does not produce any output. The sensor is able to produce small amount of signal in case of small fracture in the crystal or any other type of degradation that may be caused under specific conditions, like over-specified temperature, pressure, or vibration. These degradations generate signal with distortion, which result in false information to the controller and processor in the system. In the past few decades, there has been considerable attention focused on performing on field calibration and monitoring performance of the sensor over the time. The molecular structure of piezoelectric materials produces a coupling between electrical and mechanical domain. By definition, piezoelectricity is the electricity (electric charge) generated in a material when force (mechanical pressure) applied to it (Cady 1964).

A great amount of research efforts have been focused on monitoring resonance of a piezoelectric sensors measured by electrical impedance (Saint-Pierre et al. 1996). They propose a model to calculate the modifications of the electrical impedance due to the defects in the bonding of sensor to its structure. The sensor breakage or degradation of

electrical/ mechanical properties would change the admittance of piezoelectric material (Park et al. 2006).

Unique techniques presented by Atherton (1989), which electrically stimulate the piezoelectric sensor at the desired frequency band including resonance frequency. The electrical frequency response across capacitive load impedance is measured. This technique is used to detect mounting conditions.

There are many possible methods to perform health monitoring. The following describes the type of method used in the health monitoring. A very large amount of work exists in the field of vibration-based non-destructive evaluation (NDE) technique. Vibration based NDE has been a very active area of research for many years. Doebling et al. (1998) have published an extensive survey of over 200 papers. Lifshits and Rotem (1969) published the first vibration characteristic to identify damage to the structure. The field expanded rapidly in the 1980's.

Adams et al. (1978) first published the concept of tracking natural frequency changes for damage detection. They characterized the damage based on the ratio of frequency changes for two modes. Farrar et al. (1994) discussed limitations of monitoring the resonance frequencies. The main limitation for monitoring the health of structure is that resonance frequency is global characteristic, because it is not sensitive enough to small changes in the structure results, there is a need for very precise measurement.
Other health monitoring techniques include applying waveform transformation (Staszewski 1999), and artificial neural networks (ANN) monitoring (Worden et al. 1993), which is very costly to implement in real-life applications. One method in using ANN method is to define a damaged structure and based on correlation train the network to reject un-acceptable conditions. The waveform technique is very useful in detecting location and time of damage at the same time.

The main goal of this research is to investigate and propose a method for real-life on line field calibration with high efficiency and low cost implementation. The piezoelectric crystal is embedded inside sensor.

In order to fully implement an active sensing system, it is crucial to perform on line field calibration to measure the working condition of the sensor at desire moment. The following work summarizes the algorithm to characterize and model a piezoelectric pressure transducer. The basic concept of the method is to excite the sensor mechanically to predict some behavior, and use the results in the electronic excitation to capture the signature characteristic of the pressure transducer.

The resonance frequency monitoring method is possible by using piezoelectric crystal embedded in the structure and act as both sensor and actuator in the system. Under applied force, the piezoelectric produces an electric charge. On the other hand, when electric fields are applied to the piezoelectric, it deforms. Crawley and Anderson (1987) describe the relationship between electrical and mechanical variables.

$$S_i = s_{ij}^E T_j + d_{mi} E_m \qquad [1.1\text{-}1]$$
$$D_m = d_{mi} T_i + \varepsilon_{mk}^T E_k$$

$$\begin{bmatrix} S \\ D \end{bmatrix} = \begin{bmatrix} s^E & d_t \\ d & \varepsilon^T \end{bmatrix} \begin{bmatrix} T \\ E \end{bmatrix} \qquad [1.1\text{-}2]$$

In the equation S is the mechanical strain, T is the mechanical stress, E is the electric field, and D is charge density. Piezoelectric strain constant is d, mechanical compliance is s, and ε is the permittivity. The subscripts *i, j, m* and *k* are showing direction of stress, strain and electric field.

The method of resonance frequency monitoring uses both direct and inverse property of piezoelectric at the same time to obtain the resonance base signature for the structure. The piezoelectric crystal embedded in the structure is excited by a sinusoidal voltage sweep. The structures deform and produce dynamic response to the vibration. The responses of the system cause an electric response in the piezoelectric crystal, which gives a lot of information regarding condition of the structure. The resonance response of the system change amplitude and frequency based on the damage to the structure and crystal. The electrical response can be analyzed to obtain information based on each application of interest. Liang et al. (1994), have discussed the relation between electrical impedance of the piezoelectric and mechanical impedance of the structure.

1.3 Overview and Contribution of Thesis

Through experimental and analytical investigation, the characteristic of a desired pressure transducer is tested. Time domain model, and frequency curve fitted model are developed. The sum of the least square method and regression analysis are the main tools in parameter estimation for curve fitted frequency model. The differential equation model of the sensor is developed based on the high frequency excitation of the sensor.

One of the goals of this thesis is to document a dynamic model for a pressure transducer currently used. The model is validated by uses in simulation to investigate the relation of sensitivity of the pressure transducer and model parameters. The model validates by comparing simulated and experimental responses. The first part of this thesis discusses base and background knowledge of the history of piezoelectric transducer, piezoelectricity, and transducer.

The second part discusses the experimental protocol followed during this research and explains parameter estimation and system identification for the pressure sensor. Moreover, a discuses of the outcome of this experiments and the tangible results of the model exhibited by the data presented.

The third part investigates the optimized damage detection based on the literature review and statistical analysis of empirical data obtained from extensive experiments.
The software implementation of the signature comparison of the sensor based on the research work on the experimental data designed. The software would be implemented in the control system.

The environment uses MATLAB/Simulink for simulation of the sensor modeling. Once the model is fully developed, tested, and optimized in the simulation environment, further experiments will confirm the agreement between the outcome of the model and the actual sensor to the same excitation. This verifies the real world performance of the model with estimated parameters.

The programming languages, such as C, C++ used to design the firmware to implant in the controller and processor. C++ is the dominant language for firmware design in industry.

CHAPTER II

PIEZOELECTRICITY

Piezoelectricity is one of the natural phenomena that make possible the changing of one form of energy to another form. By definition, piezoelectricity is the electricity (electric charge) generated in a material when force (mechanical pressure) is applied to it (Cady 1964). Piezoelectricity's history dates back to 1880 when Pierre and Jacques Curie first discovered piezoelectric effect in many materials including quartz, and tourmaline. These are naturally developed minerals. Until 1916, piezoelectricity remained as a laboratory curiosity. At that time, Paul Langevin developed first major application of piezoelectric effect in submarine detector. About the same time, the mechanical resonance properties of quartz were discovered. When properly excited by an electrical signal a quartz crystal resonates over an extreme range of narrow frequencies.

In the 1930's the "crystal" phonograph microphone came into the market. During the period of 1920-1940 was a major development on all kinds of piezoelectric devices. All of the advances contributed to establishing an entirely new method of piezoelectric device development – which is designing a material to a specific application. From then to the present one of the major research areas is the application of piezoelectricity and

search for the perfect piezo product. One major application that has received numerous scientists' attentions around the world is the Health Monitoring application (Cady 1964).

2.1 Generating Piezoelectricity

A detailed analysis of the factors involved in piezoelectric action is beyond the scope of this thesis. However, the following explanation will give you an understanding of the basic process.

Material in crystal state is normally not made of molecules. Usually the matter exists as ions, particles having either a negative or positive charge. When no force is applied across the crystal, the total numbers of positive and negative charges are equal, so the crystal is electrically neutral.

In material having piezoelectric properties, the ions move easily along some axis than others. Force results in a displacement of ions such that opposite faces of the crystal would have opposite electrical charges. When the crystal complete through high impedance, these charges flow, resulting in a measurable electric current.

When a charge is applied to a crystal with piezoelectric properties, the electrical pressure causes the change of the crystal shape (Cady 1964).

2.2 Electromechanical Coupling

Piezoelectric materials can generate an electric charge with the application of force. They also can change their physical dimensions with the application of electric charge. One of the most important properties of piezoelectric materials is the ability to convert electrical energy into mechanical energy, and vice versa, which is expressed by electromechanical coupling.

Under the applied force to a single piezoelectric crystal, part of the applied force converts to an electric charge, which appears on the opposite sides of the crystal. This charged piezoelectric crystal is equivalent to a charged capacitor. The balance of the applied force is converted into mechanical energy, the same as in the case of a compressed spring. When the force is removed from the crystal, it will spring back to its original shape and the electric charge across it will disappear. A key aspect of resonance base monitoring is the use of the piezoelectric crystal as a sensor and actuator at the same time. The method utilizes high frequency structural excitation, which is typically higher than 50KHz. The piezoelectric crystal requires very low voltage to produce high frequency excitation in the structure.

The foundation of this active sensing technology is the energy transfer between the actuator and its host mechanical system. Liang (1994) showed that the electrical admittance $Y(\omega)$, which is an inverse of electrical impedance of the piezoelectric (PZ) crystal, relate directly to the mechanical impedance of actuator $Z_a(\omega)$, and its host mechanical structure $Z(\omega)$. A brief introduction of the concept is represented, which is directed closely from Liang work.

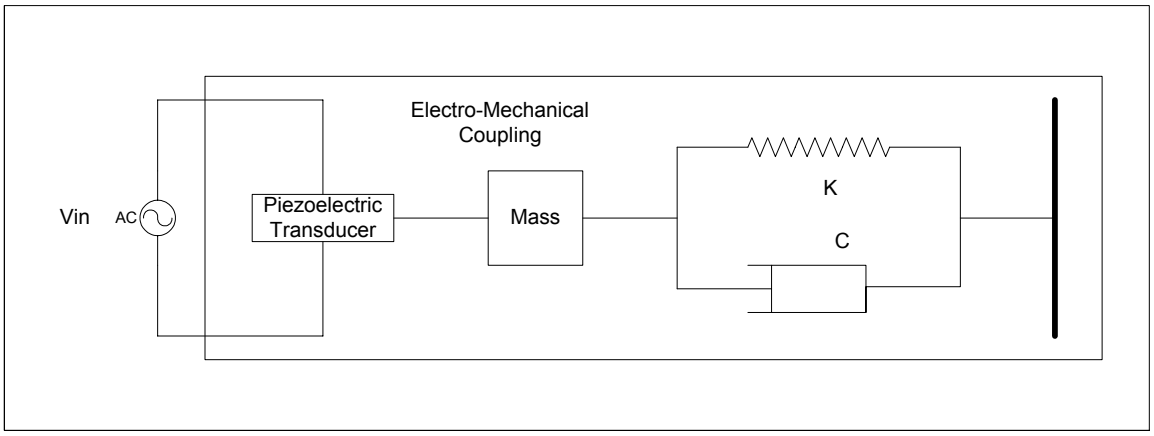

Figure 1: Electro-Mechanical Coupling of Piezoelectric Pressure Transducer

The dynamic response of the piezoelectric sensor described by the impedance method is as follows: the dynamic output characteristics of the actuators and the dynamic characteristic of the structure govern the interactions between actuators and structures. The force relation for the piezoelectric actuators express as:

$$F = K_A(X - X_i) \qquad [2.2\text{-}1]$$

Where F is the force exerted by the actuator, K_A is the static stiffness of the piezoelectric transducer, X is the displacement, and X_i is the free induced displacement of the actuator.

$$K_A = Y_{22}^E w_A h_A / l_A \qquad [2.2\text{-}2]$$

Where $w_A, h_A, and l_A$ are the width, thickness, and length of the piezoelectric transducer respectively. Y_{22}^E is the complex modulus of piezoelectric transducer at zero electric field.

$$X_i = d_{32} E l_A \qquad [2.2\text{-}3]$$

Where E is the electric field, d_{32} is the piezoelectric constant. Based on the concept of mechanical impedance we can look at structure as the spring mass damper system with following relation:

$$F = -Z\dot{x} \qquad [2.2\text{-}4]$$

Where Z is the mechanical impedance of structure:

$$Z = c + m(\frac{\omega^2 - \omega_n^2}{\omega})j \qquad [2.2\text{-}5]$$

Where c is the damping coefficient, m is the mass, K_s is the spring constant, and ω is the excitation frequency.

With harmonic steady state excitation:

$$\dot{x} = \omega x j \qquad [2.2\text{-}6]$$

The resonance frequency of structure is ω_n given by:

$$\omega_n = \sqrt{K_s / m} \qquad [2.2\text{-}7]$$

The force displacement for structure is expressed as:

$$F = -K_D x = -[c\omega j - m(\omega^2 - \omega_n^2)]x \qquad [2.2\text{-}8]$$

Where K_D is the dynamic stiffness.

From equation [2.2-1], and [2.2-8] the dynamic interaction force between actuator and structure determine as:

$$F = -\frac{K_D K_A}{K_D + K_A} X_i \qquad [2.2\text{-}9]$$

2.3 Coupled Electro-Mechanical Analysis

If the electric field is applied in z-direction, and assumes that piezoelectric transducer only expands in y-direction, the constitutive relation of the piezoelectric transducer becomes the following:

$$S_2 = s_{22}^E T_2 + d_{32} E \qquad [2.3\text{-}1]$$

$$D = \varepsilon_{33}^T E + d_{32} T_2 \qquad [2.3\text{-}2]$$

The equation of motion for the piezoelectric transducer vibrating in y-direction is given as:

$$\rho \frac{\partial^2 v}{\partial t^2} = Y_{22}^E \frac{\partial^2 v}{\partial y^2} \qquad [2.3\text{-}3]$$

Where ρ is the density of the piezoelectric transducer, v is the displacement in y-direction, and Y_{22}^E is the complex modulus of piezoelectric transducer at zero electric field. The solution to the equation is:

$$v = ve^{j\omega t} = (A\sin ky + B\cos ky)e^{jwt} \quad [2.3\text{-}4]$$

Where

$$k^2 = \omega^2 \rho / Y_{22}^E \quad [2.3\text{-}5]$$

The coefficient A can be solved as:

$$A = \frac{d_{32}E}{k\cos(kl_A) + \frac{s_{22}^E zj\omega}{w_A h_A}\sin(kl_A)} \quad [2.3\text{-}6]$$

The mechanical impedance of the piezoelectric transducer is the ratio of the excitation force to the velocity response, which is expressed as:

$$A = \frac{Z_A d_{32}E}{k\cos(kl_A)(z_A + z)} \quad [2.3\text{-}7]$$

This mechanical impedance is based on the assumption that the piezoelectric transducer has no electric coupling. The coefficient A, output displacement, stress, and strain are expressed as the following:

$$A = \frac{z_A d_{32}E}{k\cos(kl_A)(z_A + z)} \quad [2.3\text{-}8]$$

The output displacement:

$$x = \frac{Z_A d_{32} E l_A \tan(kl_A)}{Z_A + Zkl_A} \quad [2.3\text{-}9]$$

The stress:

$$T_2 = (\frac{Z_A(\cos(ky))}{(Z_A + Z)(\cos(kl_A))} - 1) d_{32} Y_{22}^E E \qquad [2.3\text{-}10]$$

The strain:

$$s_2 = \frac{Z_A d_{32} E \cos(ky)}{(Z_A + Z)\cos(kl_A)} \qquad [2.3\text{-}11]$$

The electric displacement field:

$$D_3 = \frac{Z_A Y_{22}^E d_{32}^2 E \cos(ky)}{(Z_A + Z)\cos(kl_A)} + (\varepsilon_{22}^E - d_{32}^2 Y_{22}^E) E \qquad [2.3\text{-}12]$$

The electric current is calculated by:

$$I = \overline{I} e^{j\omega t} \qquad [2.3\text{-}13]$$

Where [2.3-14]

$$\overline{I} = j\omega \overline{E} w_A l_A (\frac{d_{32}^2 Y_{22}^E z_A \tan(kl_A)}{(Z_A + Z)(kl_A)} + \varepsilon_{33}^T - d_{32}^2 Y_{22}^E) \qquad [2.3\text{-}15]$$

The electric field, $E = V / h_A$, and the admittance, $Y = I / V$ which result in:

$$Y = j\omega \frac{w_A l_A}{h_A} (\frac{d_{32}^2 Y_{22}^E z_A}{Z + Z_A} \frac{\tan(kl_A)}{kl_A} + \varepsilon_{33}^T - d_{32}^2 Y_{22}^E) \qquad [2.3\text{-}16]$$

In the frequency range of interest in most applications for the piezoelectric transducer $\frac{\tan(kl_A)}{kl_A}$ is close to one the previous equation may simplify as:

$$Y = j\omega \frac{w_A l_A}{h_A}(\varepsilon_{33}^T - \frac{Z}{Z+Z_A} d_{32}^2 Y_{22}^E) \qquad [2.3\text{-}17]$$

This equation is the groundwork for using resonance-based monitoring for in line calibration of the piezoelectric transducer. Consequently, any changes in the electrical impedance signature are considered as an indication of changes in the system condition. The variation in the electrical impedance over a range of frequencies is similar to that of the frequency response functions of a structure, which contains vital information regarding the sensor's condition.

CHAPTER III

TRANSDUCER

One of the major applications of piezoelectricity is in transducers. A transducer is any device that converts one type of energy to another for various purposes. The pressure sensor is a type of transducer.

3.1 High and Low Impedance

The piezoelectric transducer divides into two classifications: high and low impedance. High impedance units have a charge output, which requires a charge amplifier or external impedance converter for charge-to-voltage conversion. Low impedance types use the same piezoelectric sensing element as high impedance units and incorporate a miniaturized built-in charge-to-voltage converter. Low impedance types require an external power supply coupler to energize the electronics and decouple the subsequent DC bias voltage from the output signal. The piezoelectric used for this experiment is classified as high impedance and a charge amplifier converts charge to voltage. The model of the circuit has been developed for analysis and understanding the behavior of the device.

The charge amplifier converts generated charge from the piezoelectric pressure transducer to voltage. The first stage is converting charge to voltage, and second stage is a differential amplifier, which eliminates noise in the system. The third and fourth stages are low pass and high pass filter respectively. The gain for each stage and overall system is shown in the following graph.

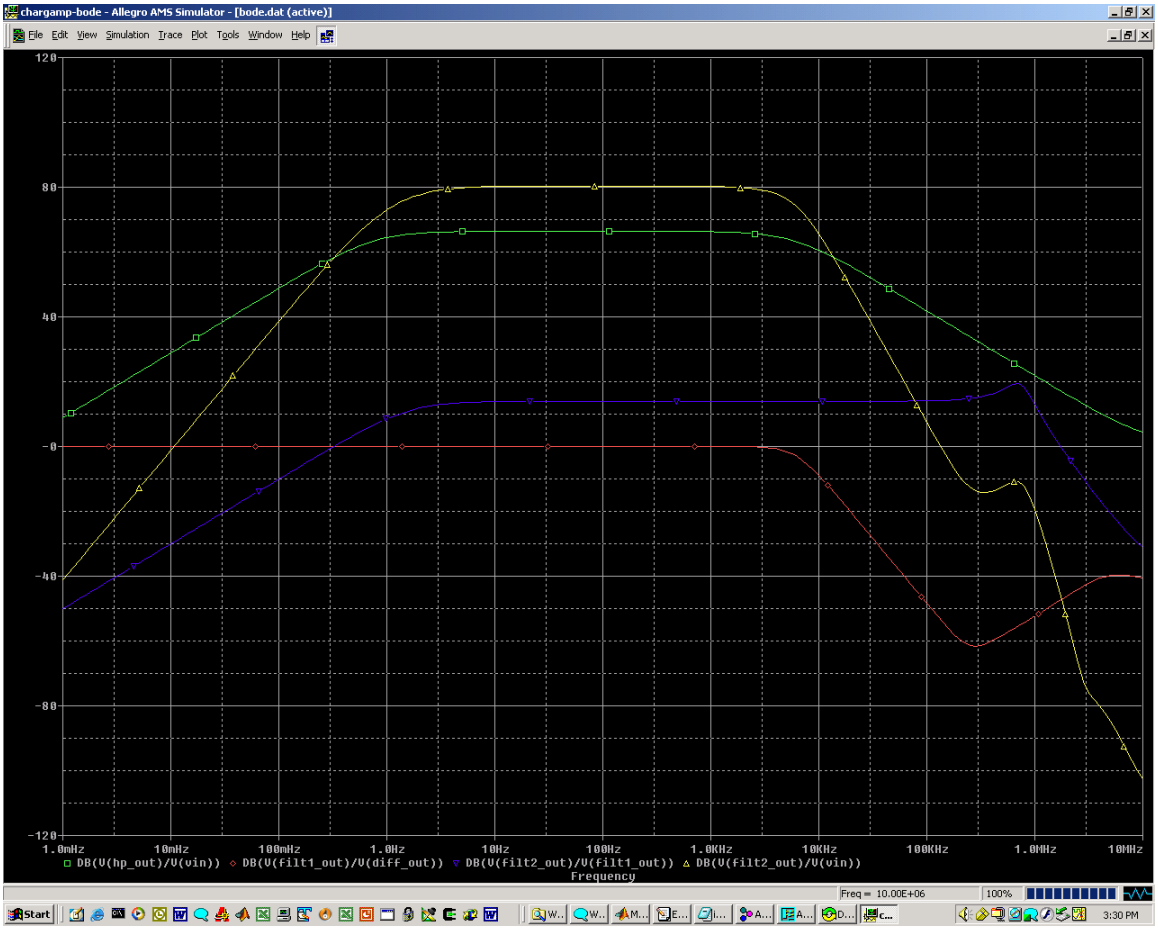

Figure 2: Bode Plot of each Stage, and Gain of Charge Amplifier System

3.2 Piezoelectric Pressure Transducer

Piezoelectric Pressure Sensors rely on the piezoelectric effect to generate a useful output signal to measure dynamic pressures. They are generally not suited for static pressure measurements. Dynamic pressure measurements under varying conditions may require sensors with special capabilities.

3.2.1 Types of Pressure Sensors

This paper describes two major modes of operation for pressure sensors manufactured in the industries. The first is a voltage mode-type sensor that has built-in microelectronic amplifiers, which converts the high-impedance charge into a low-impedance voltage output. The second type, used in this experiment research, is a charge mode pressure sensor that generates a high-impedance charge output. The charge amplifier circuit is developed to convert high-impedance charge output to a low-impedance voltage output. Charge mode quartz pressure sensors may be used at higher temperatures than voltage mode-type sensors.

3.2.2 Measuring Dynamic Pressure

The quartz crystals of a piezoelectric pressure sensor generate a charge when pressure is applied. However, even though the electrical insulation resistance is very large, the charge eventually leaks to zero. The rate at which the charge leaks back to zero is dependent on the electrical insulation resistance.

In a charge mode pressure sensor used with a voltage amplifier, the leakage rate is fixed by values of capacitance and resistance in the sensor, by low-noise cable and by the external source follower voltage amplifier used. In this case, the charge mode pressure

sensor used with a charge amplifier, the electrical feedback resistor and capacitor in the charge amplifier fix the leakage rate.

CHAPTER IV

CHARACTERIZATION, MODELING, AND PARAMETER ESTIMATION

When the crystal in a piezoelectric pressure sensor stresses, a charge generates. This high-impedance output must be routed through a special low-noise cable to an impedance-converting amplifier. High insulation resistance must maintain in the cables and connections. In this chapter, the behavior of the pressure transducer is investigated under varieties of force input. The model is represented in the form of a differential equation. The model then validates by comparing simulated and experimental responses. Sets of experiments are performed to investigate the sensor's behavior.

Moreover, the experimental protocols followed during this research are discussed. Parameter estimation and system identification for the sensor is performed. Once the model is fully developed, tested, and optimized in the simulation environment, further validation is presented in the form of extensive experiments that confirm the agreement between the outcome of the model and the actual sensor to the same excitation. This verifies the real world performance of the model with estimated parameters.

In this chapter, the dynamic characteristic of the pressure transducer is investigated extensively. Two general models for piezoelectric pressure transducers are presented. The first one is an electromechanical model of a piezoelectric transducer, and the second one is the electrical model.

4.1 Experimental Test Setup, and Procedure

There is a great interest in the engineering community to develop a field calibration technique concerning piezoelectric pressure sensors to reduce cost and improve reliability. In order to ensure those piezoelectric pressure sensors are free from unnecessary errors, the time interval between calibrations should not exceed one year. Calibrations that are more frequent should be performed if a pressure sensor is used at temperatures beyond its rated limits. Sensor disassembly for calibration in the field is very costly.

Most laboratory calibrations are performed using mechanical excitation applied to the pressure transducer while measuring electrical output. The challenge is to develop a method to perform field calibration. The principle of this work is to apply an electrical signal to the pressure sensor to measure and analyze the characteristics of the output signal for future comparison. Usually, this calibration is sufficient to verify that the performance characteristics of the pressure sensor have not changed and that it is in good operating condition. The goal of this section is to perform sets of experiments to investigate behavior and characteristics of the sensor.

4.2 The System Identification

It is desired to design and develop a method to excite crystal sensors with electrical signal at its natural vibration. Then, based on the electromechanical properties of the crystal, we would like to listen and capture the vibration signature. In order to understand the device, the following examinations have been performed. System identification is the procedure of obtaining a mathematical model of a system using observed data. There are different ways of system identification. Each way constructs a different form of knowledge about

the system. Modeling is a very important way of studying and understanding a system. A model is a simple representation of a system. This approximation may be more accurate in some respects, and less in others. A number of techniques have developed in recent years for model selection and parameter estimation. In every modeling, the following steps occur.

4.2.1 Collection of Information

The approach that we apply in system identification is based on the real, but laboratory-scale process. The identification process is characterized by searching for a reasonable model structure. This process cannot be fully automated. Human decision needs to be made in each part of the process with the help of interactive computing. The modeling accuracy largely depends on data collection accuracy.

4.2.1.1 Mechanical Excitation Applied to the Sensor

Pressure sensors include all transducers, sensors, and elements that generate an electrical signal proportional to pressure or changes in pressure. Pressure sensors are devices that read changes in pressure, and relay this data to recorders.

There are many technologies by which pressure transducers and sensors function. One of the most widely used technologies is piezoelectric. Other variations within pressure sensors include their manners of receiving and displaying data. Many of these sensor's output are in analog form, either current or voltage. Other methods include switches, alarm outputs, parallel or serial output to sensor systems or industrial computers, or, in some advanced pressure sensor models, digital or video displays.

The sensor used in this research project is the piezoelectric pressure transducer, which is designed for sensing dynamic pressure fluctuations, even in the presence of high static

pressure and temperature. The goal of the research is to develop an algorithm to excite the sensor by electric force, and based on that analysis the performance of the sensor is evaluated.

In order to accomplish the goal, a set of experiments is performed to investigate the sensor's behavior. The sensor hit hard in short period and the response is observed. The sensors connect to a digital storage oscilloscope TDS2000B Series, the force applies to the sensor, and a consistent response is observed.

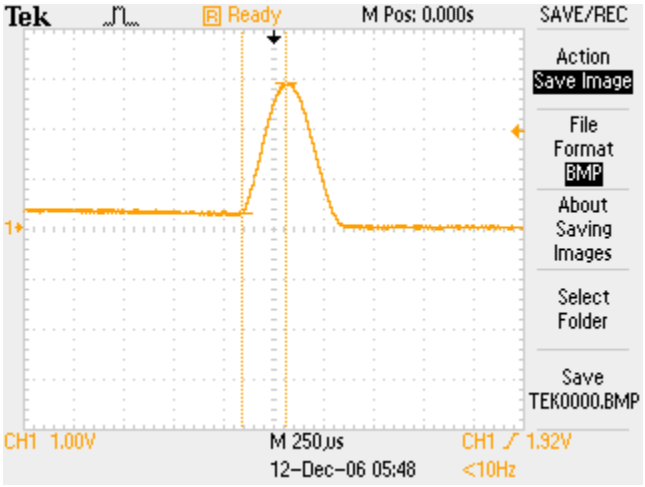

Figure 3: The Response of the Mechanical Excitation of Sensor

This is the electromechanical nature of the piezoelectric material. In general, if you deform a piezo crystal by applying a force, you will get charge separation: Think of a simple capacitor.

In material having piezoelectric properties, the ions move more easily along some axis than others. Force results in a displacement of ions such that opposite faces of the crystal would have opposite electrical charges. When the crystal is connected through high impedance, these charges flow, resulting in a measurable electric current.

4.2.1.2 *Mechanical Excitation Observation through Charge Amplifier*

Next, the sensor connected to the designed charge amplifier to observe the out put signal resulting from hitting the sensor mechanically.

The sensor connects to the charge amplifier and force is applied to the sensor. The output signal is going through a charge amplifier for conversion and amplification. The distortion is due to the charge amplifier, and we observe ringing in the response. The cause of the unclear ringing response is due to the response of the pressure transducer or charge amplifier, which more experiments is performed.

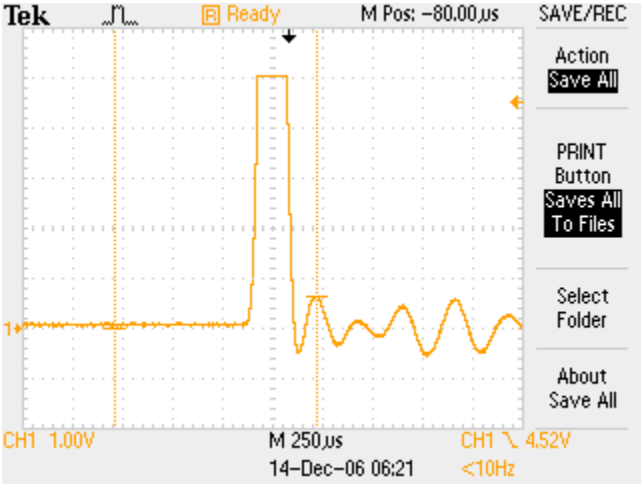

Figure 4: The Respond of the Mechanical Excitation of the Sensor through Charge Amplifier, the Distortion is due to the Saturation of Charge Amplifier

4.2.1.3 *Charging and Discharging of the Device*

We first focused on designing a charge injection device to apply charge to the sensor and observe the response. Due to the fact that this research is conducted with an eye toward

more understanding of the sensor for field calibration of industrial applications, the charge responding of the sensor was considered first. In order to accomplish this goal, a simple charge injection circuit is designed.

It is required that the charge injection circuit accommodates the following requirements in order for the design to be viable. The capacity of crystal is *175 pF*, and the operating pressure for the crystal is *30*-psi normal dynamic range. Because, the charge amplifier saturates at *10 V*, no voltage higher than that is recommended for circuit application. On the other hand, the applied voltage to the sensor to operate in normal limits needs to be calculated.

$$q = c \times v \rightarrow v = \frac{q}{c} \rightarrow \frac{17\,pC \times 30}{175\,pF} = 2.88V \qquad [4.2\text{-}1]$$

There is a sensor that is given some energy (charge). When it discharges, it deforms and releases that energy (Electrical Signal) which is captured.

A simple charge injection device is designed and built with supply voltage in the normal operating range of the sensor, and a capacitance at least 10X larger than sensor capacitance 2.2 nF , and 1-ohm resistor. A relay is used to control the switching of charging capacitance and discharging time to charge the sensor.

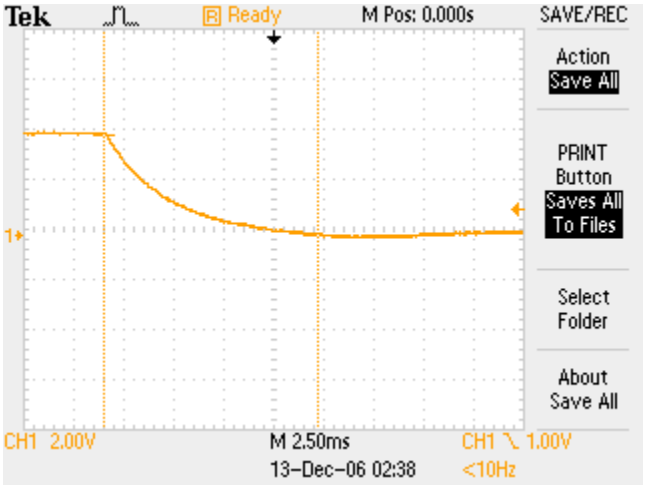

Figure 5: Charging of Pressure Sensor by Charge Injection Test Circuit

The results from this experiment confirm the capacitance property of the device, and lead us to hit the sensor hard at a short period by electrical signal to excite its resonance. We decided to generate a step signal to excite the sensor electronically, which is explained in the following sections.

4.2.1.4 Mechanical Resonance Properties

When a crystal is properly excited by an electrical signal, it vibrates (resonates) over an extremely narrow range of frequencies. The range is so narrow, in fact, that modern crystals are often accurate within 0.001%. This has led to the use of crystals as a highly stable frequency determining elements in radio communication equipment. During World War II, the United States alone used over 50,000,000 crystal elements (Wilson 2005).

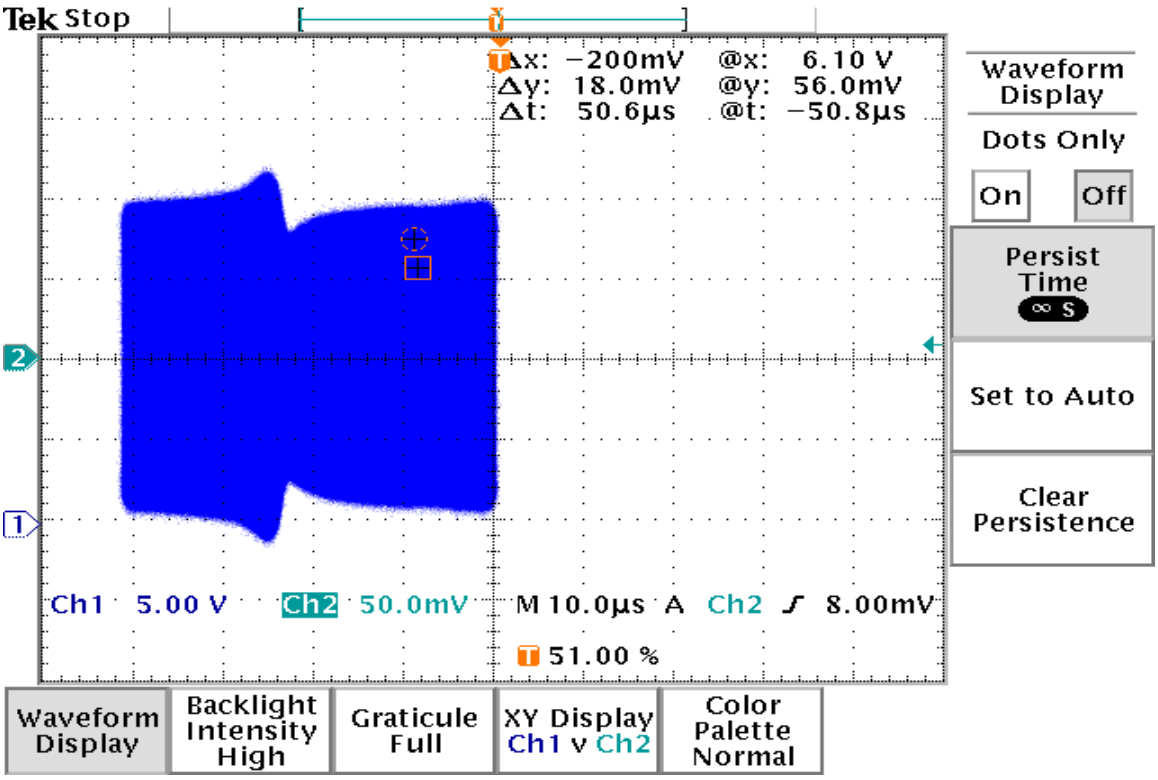

Figure 6: Frequency Response of a Pressure Transducer, X-axis Voltage Correspond to Frequency, and Y-axis Voltage Amplitude

The pressure transducer vibrates at its resonance frequency by applying an ac voltage to its piezoelectric layers. The amplitude of AC voltage is 2.8 V, to keep it between linear operation ranges. The resonance frequency is about 79 KHz. The voltage to frequency converter is connected from function generator to channel one of the oscilloscopes. Channel 1 out-put is voltage proportional to frequency. The channel 2 is representing voltage across a 500-ohm shunt resistor connected in series with the sensor. This is actually the current generated by the sensor.

4.2.2 General Modeling Structure

There are two major model structures: parametric and nonparametric. In parametric models, only a limited number of parameters are estimated through observation. We know important parts of the system. Moreover, in parametric model the physical structure of the model is determined by known physical insight. In nonparametric modes, no model is defined, and the system behavior is described by the response of the system for special excitation signal. This is suitable when we have less knowledge about the system.

4.2.2.1 Electromechanical Modeling of Piezoelectric Sensor

An accurate assumption used in mathematical modeling of electromechanical devices is that the variables in the electrical and mechanical domains linearly couple. Energy conversions between the two domains are produced by a change in the variables of the system. The linear coupling between the electrical and mechanical domains is represented by using an ideal linear transformer. This type of modeling is used to represent the piezoelectric transducer (Ikeda, 1996). The electrical quantities are shown on the left side of the transformer, and the mechanical quantities are on the right. V presents transducer voltage. The external force apply to the transducer is represented by F. It is desired to excite the piezoelectric pressure sensor (PPS) device by an electrical signal, which causes vibratory motion. Based on piezoelericity property of the sensor we can see the response by charge generation. The research and development is performed to capture the signature response.

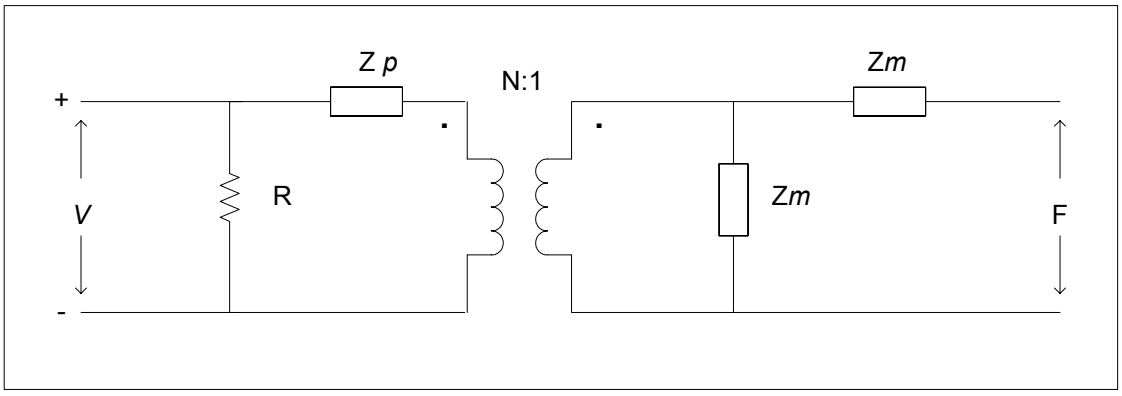

Figure 7: The Linear Coupling Between the Electrical and Mechanical Domains

4.2.2.2 *Electrical Modeling*

The equivalent electrical circuit for a general piezoelectric pressure sensor is shown in the following figure. The simplified circuit is adequate for application analysis. The electrical impedance is represented by two terms in the equivalent circuit. R represents the DC resistance, and *Z* models the ability of the sensor to store electrical charge. The capacitance of the device has been given as 175 *pf*. The piezoelectric transducer is effectively a capacitor, which produces a charge *q* across its plates proportional to a force applied to the crystal. The open circuit voltage *e* out of the transducer is equal to the generated charge divided by the transducer capacity, or E=q/C. Thus, the generator can also be represented as a voltage generator and a serious capacitance with DC resistance.

The output from the crystals is a high impedance charge. The internal components of the pressure sensor and the external electrical connector maintain a very high (typically 10 e^{13} ohm) insulation resistance. Consequently, any connectors, cables, or amplifiers used must also have a very high insulation resistance to maintain signal integrity. The least squares method is applied to estimate DC resistance based on experimental data.

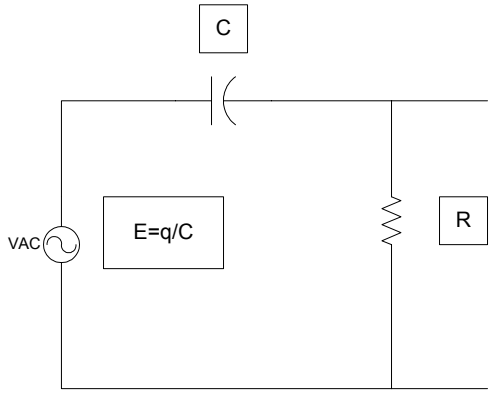

Figure 8: Electrical Model of Pressure Transducer

4.3 Parameter Identification

The goal of this section is to develop a specific model for the pressure transducer in the field to do simulation for field calibration. Parameter identification is a procedure by which a mathematical description of variable or component dynamic behavior is extracted from test data. It can be thought of as an inverse of simulation. In a parametric model, relation between inputs and outputs of a system formulate in a mathematical form. This mathematical form defines the structure of the model and set of parameters. Parameter estimation is a way to adjust the model's parameter to fit observation based on a cost function. We used experimental data in the estimation procedure to obtain optimal estimate of DC resistance (unknown parameter). The method of least squares estimation has been applied (Kirk 1998).

4.3.1 Least square Estimation

Least square estimation is a mathematical optimization technique that has been in use since the early nineteenth century. The least squares methods are applicable to both linear as well as non-linear problems. The goal of the method is to minimize the sum of the squares of the differences between points generated by the function and corresponding points in the empirical data. It requires a large number of iterations to converge. The Excell software is used for this project to perform optmization process. The application of sum of least square in this project is in the curve fitting of empirical data, and finding the best parametrs for the model.

Raol (2004) approached a model base, and defined a mathematical model of the dynamic system as following. The following approach is directed from his work.

$$z = H\beta + v, \qquad y = H\beta \qquad [4.3\text{-}1]$$

Where y is $(m \times 1)$ vector of empirical outputs, z is $(m \times 1)$ vector that denotes the measurement of the unknown parameter through H, and v is the error between empirical, output and output through the unknown parameter. The chosen estimator β should minimize the sum of the squares of the error.

$$J \cong \sum_{k=1}^{N} v_k^2 = (z - H\beta)^T (z - H\beta) \qquad [4.3\text{-}2]$$

J is cost function, and v residual errors at time k. Cost function is a measure of the model's quality. It is a function of the error between the model output and the system output. Superscript T is for the vector transposition. The minimization of J with respect to

β yields:

$$\frac{\partial J}{\partial \beta} = -(z - H\beta_{LS})^T H = 0 \quad \text{or} \quad H^T(z - H\beta_{LS}) = 0 \qquad [4.3\text{-}3]$$

After simplification, we get:

$$H^T z - (H^T H)\beta_{LS} = 0 \quad \text{or} \quad \beta_{LS} = (H^T H)^{-1} H^T z \qquad [4.3\text{-}4]$$

The form in the above equation is the best parameter estimation that is proved in the above statements. We can obtain β using the pseudo-inverse of H, $\beta_{LS} = (H^T H)^{-1} H^T z$. This shows that the estimate can be obtained from the knowledge of data.

4.3.2 Experimental Setup and Procedure

There are a lot of documents on system identification. However, the best way to explorer system identification is by working with real data. Any estimated model is a simplified reflection of reality, but is sufficient for rational decision-making. Since the system is linear, the step responses of the sensor capture and collect. The setup shown below, includes a waveform generator model Agilent 33220A to generate 2.8 Vpp step signal. A digital storage oscilloscope TDS2000B Series monitors voltage across 500 Ω, resistor.

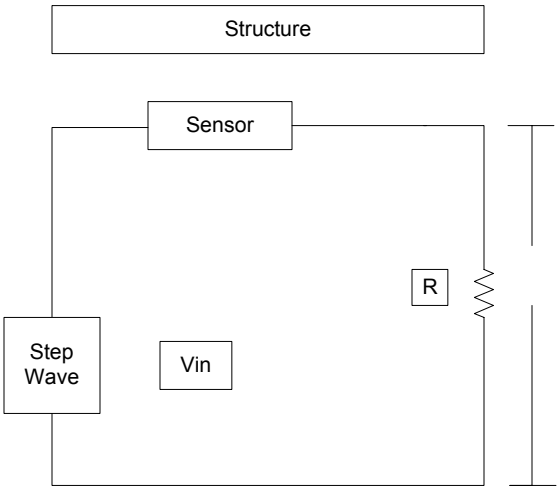

Figure 9: Experimental Setup for Capturing Step Response of Transducer

The dynamic sensor responds to the step signal's rate of change. A pulse is generated with a frequency of 1 Hz, and pulse a width of 1%, as it is shown below. The pressure transducer is charging at the rising edge and discharging at the falling edge.

In order to reduce the effect of the shunt resistor on the sensor response, the value of 20 Ω is selected for the shunt resistor.

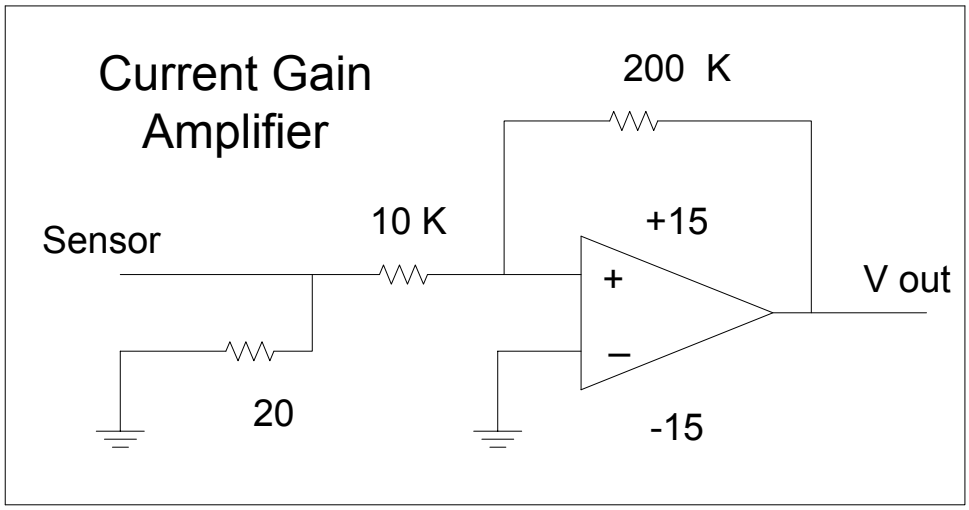

Figure 10: Current Gain Amplifier Circuit

Since the current that is generated by the sensor is very small, there is need for designing a current amplifier to increase the gain. The current amplifier circuit, as shown in the following figure, presents almost 20 Ω load impedance to the ground because the inverting input appears as a virtual ground. The input current flows through the shunt resistor (R_S), generating voltage.

$$V_{\circ} = -\frac{R_F}{R_i} \times i_s \left(\frac{R_i \times R_S}{R_i + R_S}\right) \qquad [4.3\text{-}5]$$

$$Z_{in} = \frac{Z_{op}}{1 + (Z_{op} / R_F)(1 + A)} \approx \frac{R_F}{1 + A} \qquad [4.3\text{-}6]$$

A recent study by Simmers et al. (2004) shows that every 5.5° C change in temperature results in a 1% change in capacitance of piezoelectric material. The author is currently working on the signal processing techniques to normalize the measured capacitance data

with respect to change in temperature to fully apply the proposed sensor field calibration process. The automated data processing algorithm used to measure capacitance is under development, which is required to implement the proposed concept to field application.

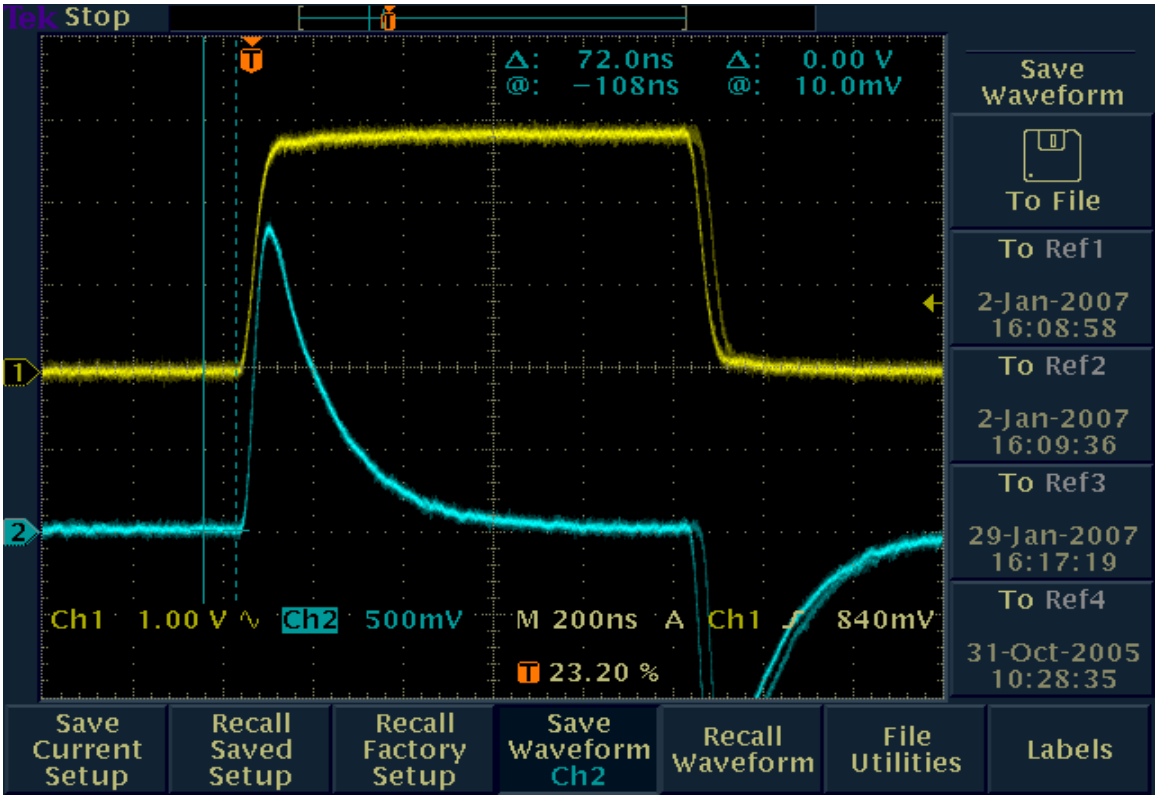

Figure 11: Step Response of the Pressure Transducer at Rising and Falling Edge

To find the DC resistance of the pressure transducer, we chose to concentrate at the rising edge and charging behavior of the pressure transducer.

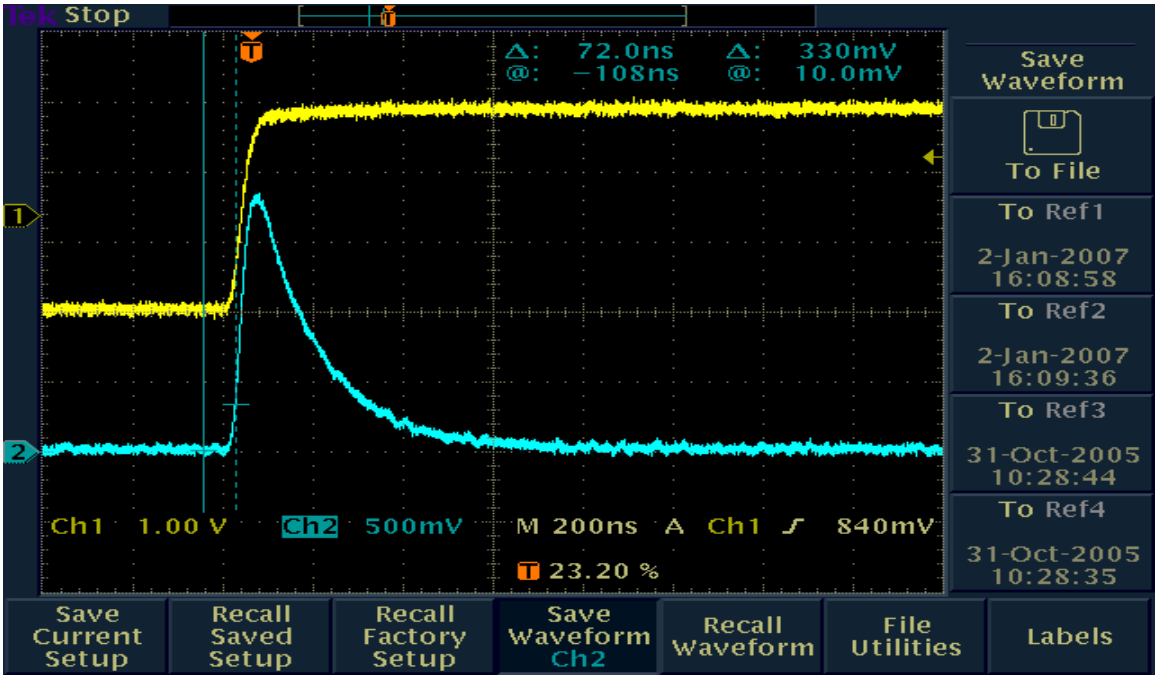

Figure 12: Step Response of the Pressure Transducer at Rising Edge (Charging)

The piezoelectric transducer is effectively a capacitor, which produces a charge q across its plates proportional to a force applied to the crystal. The open circuit voltage e out of the transducer is equal to the generated charge divided by the transducer capacity, or E=q/C. Thus, the generator can also be represented as a voltage generator and a serious capacitance with DC resistance. The charging current asymptotically approaches zero as the capacitor becomes charged. Charging the transducer stores energy in the electric field between the membranes of the sensor. The rate of charging is typically described in terms of a time constant RC which is estimator β in the least squares methods approach.

$$V_C(t) = \frac{C}{Q_0}(1 - e^{-\frac{t}{\tau}}) \qquad [4.3\text{-}7]$$

$$V_R(t) = V_0 e^{-\frac{t}{\tau}} \qquad [4.3\text{-}8]$$

$$\tau = RC \qquad [4.3\text{-}9]$$

It is desired to have a linear relationship between parameter and output, accomplished as follow:

$$\ln(V_R(t)) - \ln(V_\circ) = (-1/\tau)t \qquad [4.3\text{-}10]$$

From this equation, we find the relationship of $y = H\beta$, and $\beta = -\frac{1}{\tau}$

The least square technique is considered a deterministic approach to the estimation problem. An estimator β chose the way that minimizes the sum of the squares of the error (see section 5.3.1)

The linear squares fit has been applied to the experimental data from the step response of the transducer to find the optimal value of parameter β_{LS} =5.6036e+006, and with a capacitance of 175 *pf,* the resultant DC resistance is 1.0816 KΩ.

4.3.3 Efficiency of an Estimator

After establishing the resistance, it is important to obtain the covariance of the estimation error, which measures the quality of an estimator. First, the output through the least square parameter is calculated. Raol, (2004) defines the covariance as:

$$Y_{output} = \beta_{LS} \times H \qquad [4.3\text{-}11]$$

$$Error = Y - Y_{output} \qquad [4.3\text{-}12]$$

$$\mathrm{cov}(Error) = \sigma^2 (H^T H)^{-1} \qquad [4.3\text{-}13]$$

The calculated value for the covariance was 0.0028. The standard deviation of the estimation error is calculated by Matlab as 1.14e-006. This value, which is close enough to zero, validates the quality of the estimator.

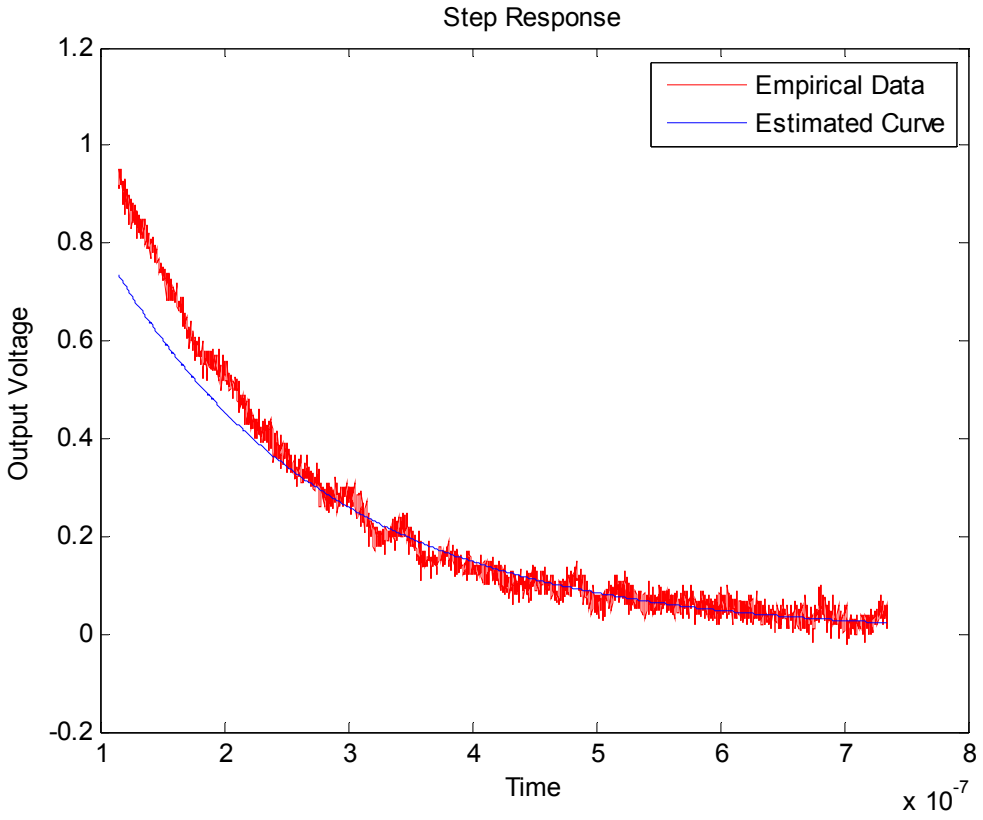

Figure 13: Graph of Empirical Data (Red), and Data from Equation by Parameter Estimation (Blue).

4.4 Modeling in Time Domain

The goal is to develop a specific model for the pressure transducer to do simulation for the field calibration. The step response of the process is given in the previous graph.

It reveals that the dynamic is simple. The minimum rising time achieved by the function generator was 5 ns. The step response equation is presented as follow:

$$V_R(t) = 1.4e^{-5.6036e+006t} \qquad [4.4\text{-}1]$$

A continuous-time LTI system is completely characterized by its impulse response *h* (t) as described through the convolution operation as follows:

$$y(t) = \int_{-\infty}^{+\infty} x(\tau)h(t-\tau)d\tau \qquad [4.4\text{-}2]$$

This equation defines the convolution of two continuous time signals x(t) and *h* (t), denoted by :

$$y(t) = x(t) * h(t) = y(t) = \int_{-\infty}^{+\infty} x(\tau)h(t-\tau)d\tau \qquad [4.4\text{-}3]$$

There is a fundamental result that the output of any LTI system is the convolution of the input *x*(t) with the impulse response *h* (t) of the system.

Also, there is a close relationship, between the unit step function *u*(t-a) and the unit Impulse $\delta(t-a)$. In particular, the unit step function is the integral of the unit impulse, or

$$u(t-a)=\int_{-\infty}^{t}\delta(\xi-a)d\xi \qquad [4.4\text{-}4]$$

The following closely followed by (Meirovitch, 1986) work. ξ is merely a variable of integration, which results from the fact that unit impulse is the time derivative of the unit step function:

$$\delta(t-a)=\frac{du(t-a)}{dt} \qquad [4.4\text{-}5]$$

The relationship, between the unit impulse $\delta(t)$ and the impulse response $g(t)$ in the symbolic form is written as:

$$\mathrm{D}[\,g(t)\,]=\delta(t) \qquad [4.4\text{-}6]$$

where D is the differential operator. Integrating the above equation with respect to time and assuming that the differentiation and integration process are interchangeable, and we obtain:

$$\int_{-\infty}^{t}D[g(\xi)]d\xi=D\left[\int_{-\infty}^{t}g(\xi)d\xi\right]=\int_{-\infty}^{t}\delta(\xi)d\xi \qquad [4.4\text{-}7]$$

The relationship between the unit step function *u(t),* and the step response *s(t)* has the symbolic form.

$$D[s(t)]=u(t) \qquad [4.4\text{-}8]$$

We can conclude from both equations that

$$s(t) = \int_{-\infty}^{t} g(\xi) d\xi \qquad [4.4\text{-}9]$$

The step response is the integral of the impulse response or impulse response in the differential of step response.

We obtain the impulse response of the sensor by calculating a differential of the step response as follows:

$$V_R(t) = -7.84504 e^{-5.6036e+006t} \qquad [4.4\text{-}10]$$

The Bode plot of the system is given in the next graph. It reveals that the dynamic is simple. The magnitude of the Bode plot is a rising line with slope of 20 db per decade.

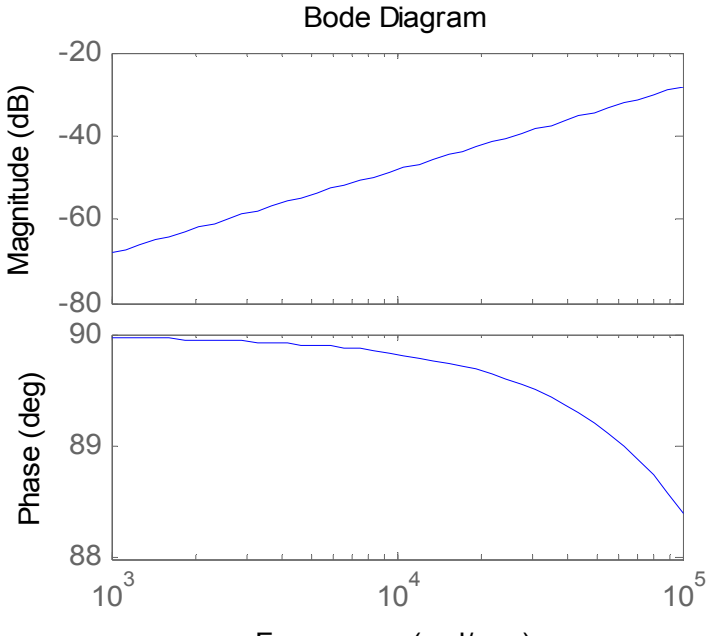

Figure 14: The Bode Plot of the Sensor, Obtained from Time Domain Modeling

4.5 Modeling in Frequency Domain

The transfer function of a system provides a summary of the input/output response and it is very useful for analysis and characterization the system. We can build an input/output model by directly measuring the frequency response and fitting a transfer function fit to it.

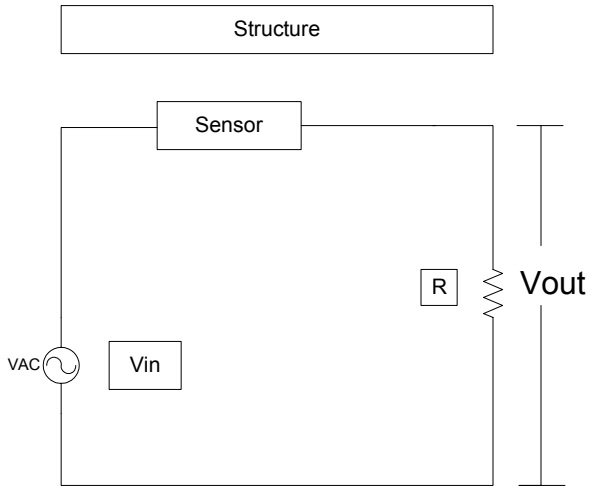

Figure 15: Experimental Setup for Frequency Response of Transducer

4.5.1 Experimental Setup and Procedure

The setup shown in Figure 16, includes waveform generator model Agilent 33220A to generate a 2.8 Vpp Sine wave signal. Voltage across a 20 Ω resistor is monitored by a digital storage oscilloscope TDS2000B Series. The current amplifier design in section 4.4 is used to increase gain by a factor of 20.

4.5.2 Frequency Response

In real-life situations, such as modeling transfer functions from physical data, frequency response has certain advantages. The frequency response is a representation of the system's response to sinusoidal inputs at varying frequencies. The output of a linear system to a sinusoidal input is a sinusoid of the same frequency but with a different magnitude and phase. To build an input/output model of the pressure transducer, the input to the system is perturbed by using a sinusoidal signal at fixed frequency. When a steady state is reached, the amplitude ratio and phase lag gives the frequency response for the excitation frequency (6). The complete frequency response obtained by the excitation voltage of 2.8 Vpp, sweeping over a range of 1KHz-100 KHz of frequencies as shown in the graph in Figure 16.

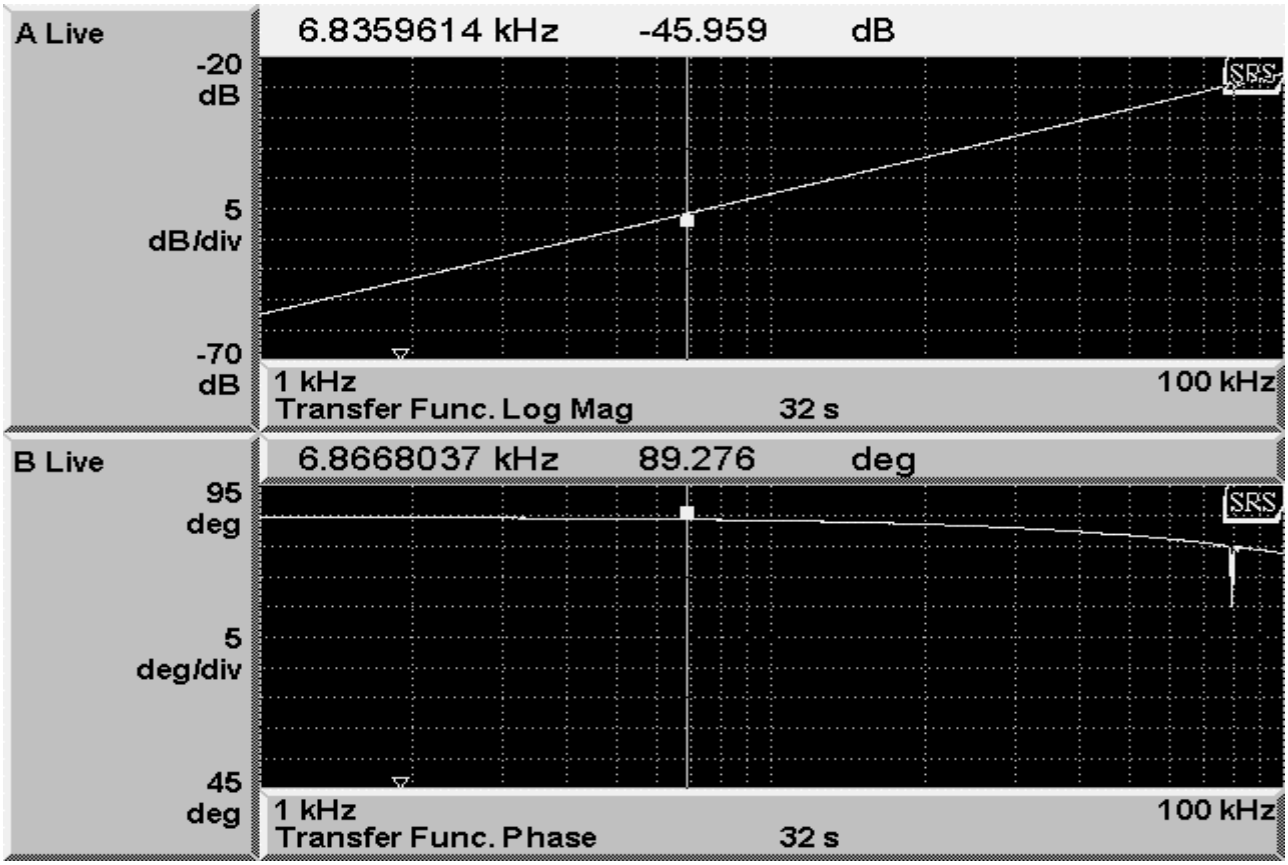

Figure 16: Frequency Response of the Pressure Transducer. The Input is the Voltage to Excite the Sensor

By using correlation techniques, the frequency response can be obtained. The spectrum analyzer device is used to obtain the frequency response of the pressure transducer accurately.

4.5.3 Transfer Function

The mathematical relationship between the input and output of a system is represented by the transfer function. The transfer function is used mostly in the analysis of single-input

single-output linear time invariant (LTI) system. LTI system theory, which investigates the response of a LTI system to an arbitrary input signal, is used to describe a system. Any system that can be modeled as a linear homogeneous differential equation with constant coefficients is an LTI system. Examples of such systems are electrical circuits made up of resistors, inductors, and capacitors (RLC circuits). A pressure transducer system is also an LTI system, and is mathematically equivalent to RLC circuits at low frequency. The goal of this section is to obtain a differential equation model based on empirical data of the frequency response of the system.

As shown, the system has a characteristic about 75-85 KHz. The Bode plot of the system for frequency ranges between 60kHz-100kHz is obtained to observe the characteristic of the system. The rest is a straight line with a slope of 20 DB per decade.

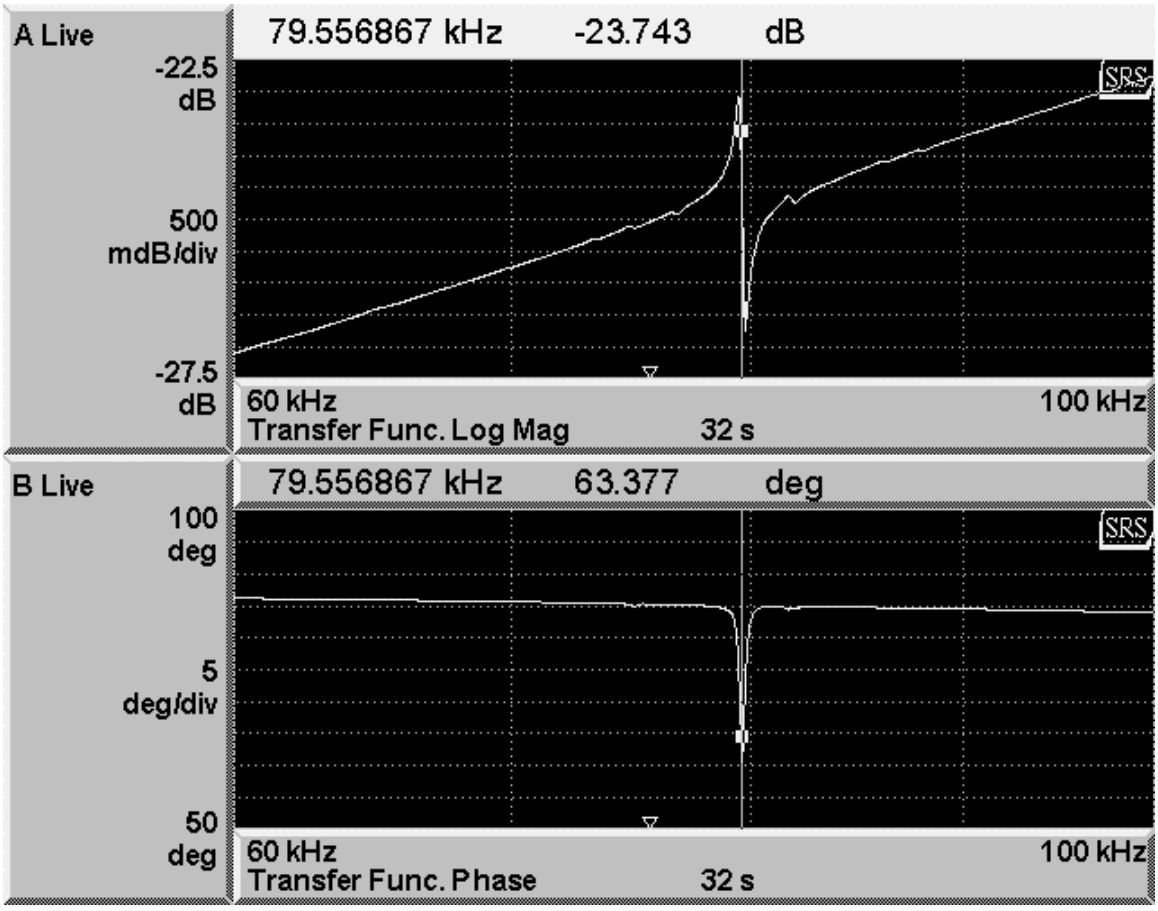

Figure 17: The Bode Plot of the Pressure Transducer

4.5.4 Model Structure Selection

The choice of an appropriate model structure is very important for a successful identification application. The behavior of the system is like a harmonic response for two masses in a spring damp system. The least squares fitting procedure described previously have been used in Excel with regression analysis to perform curve fitting for the empirical data of the frequency response of the system. The equation appears below in two parts, real and imaginary. The curve fitted frequency model of the system can be written as follows:

$$Y_{real} = -\frac{A\left(1-\left(\frac{F}{F_1}\right)^2\right)}{\sqrt{\left(1-\left(\frac{F}{F_1}\right)^2\right)^2+\left(2\xi_1\left(\frac{F}{F_1}\right)\right)^2}} + \frac{A\left(1-\left(\frac{F}{F_2}\right)^2\right)}{\sqrt{\left(1-\left(\frac{F}{F_2}\right)^2\right)^2+\left(2\xi_2\left(\frac{F}{F2}\right)\right)^2}}$$

[4.5-1]

$$Y_{image} = +\frac{A\left(2\xi_1\left(\frac{F}{F_1}\right)\right)}{\sqrt{\left(1-\left(\frac{F}{F_1}\right)^2\right)^2+\left(2\xi_1\left(\frac{F}{F_1}\right)\right)^2}} - \frac{A\left(2\xi_2\left(\frac{F}{F_2}\right)\right)}{\sqrt{\left(1-\left(\frac{F}{F_2}\right)^2\right)^2+\left(2\xi_2\left(\frac{F}{F_2}\right)\right)^2}} + C_{imag}F$$

[4.5-2]

$$H(F) = 20\log\sqrt{\left(Y_{real}{}^2 + Y_{image}{}^2\right)} \qquad [4.5\text{-}3]$$

Natural frequencies F_1, and F_2 are very close (3Hz differences in 1KHz-100KHz range), and they follow each other, the same is true for damping ratios ξ_1 and ξ_2.

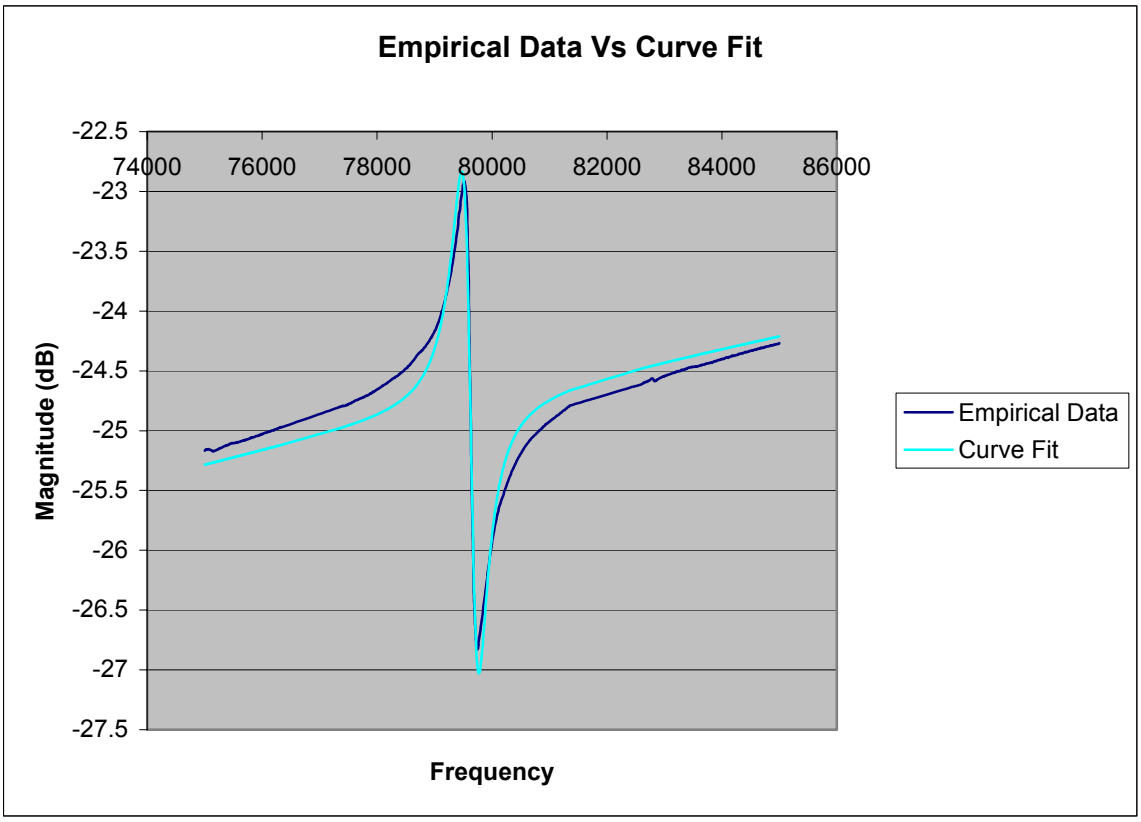

Figure 18: Magnitude of the Frequency Response of the Empirical Data (Dark Blue) vs. Curve Fitted Data (Light Blue)

The magnitude is $-20\log(\sqrt{real^2 + imaginary^2})$. Then, by substituting *s=jw*, for frequency in *(f/f1),* and *(f/f2)* terms and after simplification we would get:

$$H(S) = \frac{(1.4286e{+}006)S^3 + (5.9271e{+}008)S^2 + (9.0857e{+}015)S}{S^2 + 477S + 632e7} \qquad [4.5\text{-}4]$$

$$H(S) = \frac{Y(S)}{X(S)} \qquad [4.5\text{-}5]$$

$$(1.4286\text{e}{+006})\frac{\mathrm{d}^3 y}{dt^3}+(5.9271\text{e}{+008})\frac{\mathrm{d}^2 y}{dt^2}+(9.0857\text{e}{+015})\frac{\mathrm{d}y}{dt}=\frac{\mathrm{d}^2 x}{dt^2}+477\frac{\mathrm{d}x}{dt}+632\text{e}7$$

[4.5-6]

The Bode plot of the system from the differential equation model obtain, which confirm close enough parameter estimation.

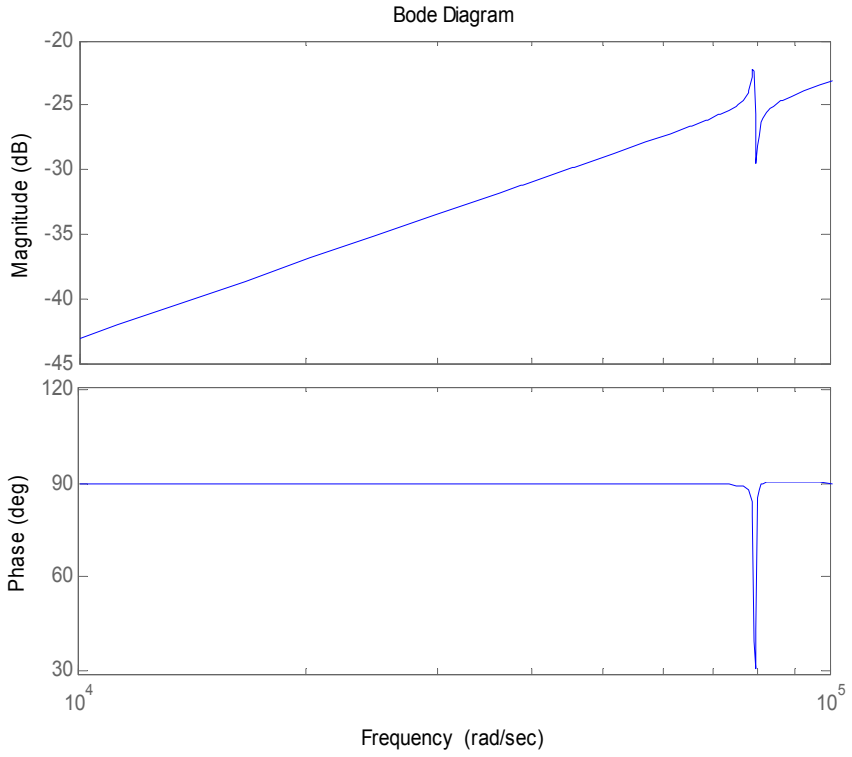

Figure 19: Bode Plot of the System from the Differential Equation Model

The Matlab was used to capture a Bode plot of the system. In Figure 19, the upper graph shows the magnitude of impedance and the lower graph phase.

4.5.5 Resistive Shunting and Damping Characteristic

A shunting resistor is used in the experiment to monitor resonance characteristic dissipate energy and may effect the damping characteristic. In order to demonstrate the effectiveness of the shunting resistor value on the damping characteristic, experiments with a series of different resistors were performed. The frequency at which peak damping is observed is related to the inverse of RC, time constant of shunt circuit.

The value of resistors in the experiments is 10, 50, 60, 70, 100, and 150 ohms. Experimental results obtained with piezoelectric sensor connected in series with each of these resistors. The data were collected, and plotted at the same time in the following graph.

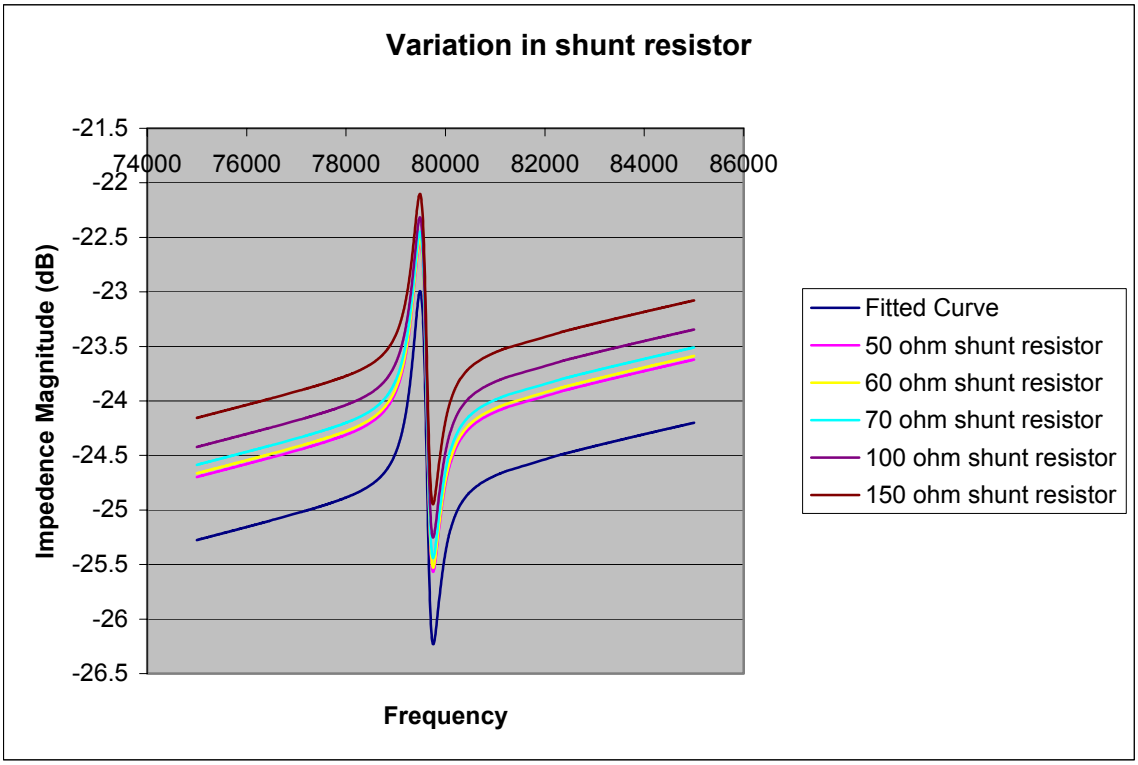

Figure 20: Effect of Shunt Resistor on the Damping and Resonance Characteristic

These results demonstrate that the shunt resistor does not have significant effect on the damping characteristic, but as the value of shunt resistor increases, the gain increases as well.

CHAPTER V

FIELD CALIBRATION TECHNIQUE FOR PIEZOELECTRIC SENSOR

Even with an extremely detailed model, the real system may contain unknown or slowly changing physical parameters. Thus, the controller has to account for changing parameters and the affects such changes would have on the system response. Heavy simulation can serve as preliminary examination of how changing parameters may affect the frequency model of the pressure transducer. More over, there is great interest in the ability to monitor a structure and detect damage and predict life time (Prognosis). Research in resonance based damage identification has been rapidly expanding over the last few years. The basic idea behind this technology is that natural frequency functions as a physical property of a system as do mass, damping, and stiffness. Therefore, any change in physical properties will cause detectable changes in the resonance frequency characteristic.

5.1 Correlation of the Model Parameters and Resonance Characteristic

The frequency model for selected parameter variations was heavily simulated. The variation in changes of resonant frequency characteristic by parameter variations of the

model was also examined. Since each pressure transducer is unique based on the piezoelectric crystal that the structure contains, at the beginning of operation the system run and the hardware capture the respond, and any desired time calibrations that are more frequent perform and comparison analysis obtain to conclude working condition of the pressure transducer. For example, if a pressure sensor is use at temperatures beyond its rated limits, the testing and comparison analysis is performed by considering expected variation based on behavior of the system for slight changes in each parameter. It is crucial to understand the parameters variations with relation to the resonance characteristic. We would like to quantify the sensitivity of the response to each parameters variation for the models.

This section presents the results of a study of the effect of variations of systemic parameters on the frequency model response of the dynamic analysis. The systemic parameters are A, natural frequency, damping ratio, and Cimage (capacitance impedance). Each of these parameters varies one at a time while the other values remain constant. For each variation of parameters, a set of curves is obtained.

5.1.1 Variation in Parameter *A*

This parameter ***A*** factor, along with damping ratio, determines the amplitude of the natural frequency phenomena. The value changes in increasing and decreasing order. The curve obtained is compared to the empirical data curve in each situation. As the values increases, the amplitude becomes higher and sharper. The amplitude becomes smaller as the value of A decreases. The summary of results appears in Figure 21.

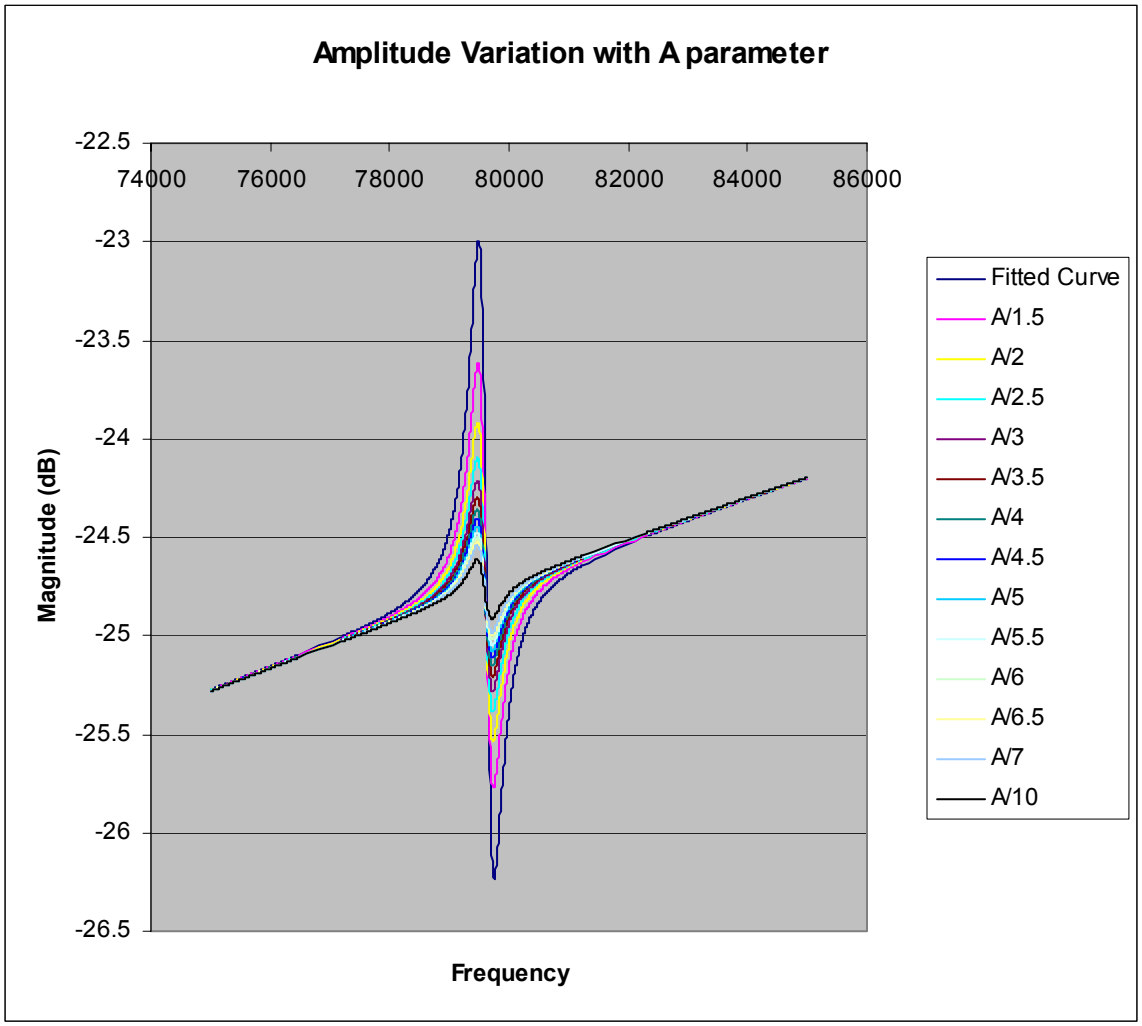

Figure 21: The Plot of Empirical Data and Frequency Model for Parameter A in Decreasing Order

5.1.2 Variation in Natural Frequency Parameter

Figure 22 shows the summary of the variation results for frequency model plot for the empirical data. The natural frequency parameter influences various factors. The system

has very low differences between F1, and F2, which is approximately 3 Hz in ranges of 1 KHz-100 KHz. They follow each other in any variations. Hence, no comment can be made about the dependence of two natural frequencies; it seems that this relationship is characteristic of the system. It can be observed through extensive experiments of the variation of the natural frequency parameter, that the model either shifts to the left or to the right. For the increasing value of the natural frequency, the curve shifts to the right. For the decreasing value of the natural frequency, the curve shifts to the left.

These results indicate that, we can use it to characterize the behavior of the system. Any factor that affects a change in the natural frequency of the sensor can be observed through a predicted value of the frequency model. The piezoelectric element can be electrically stimulated in the pressure transducer in the diagnostic frequency band, which is different than normal operation band, and measuring the electrical frequency respond characteristic of the natural frequency.

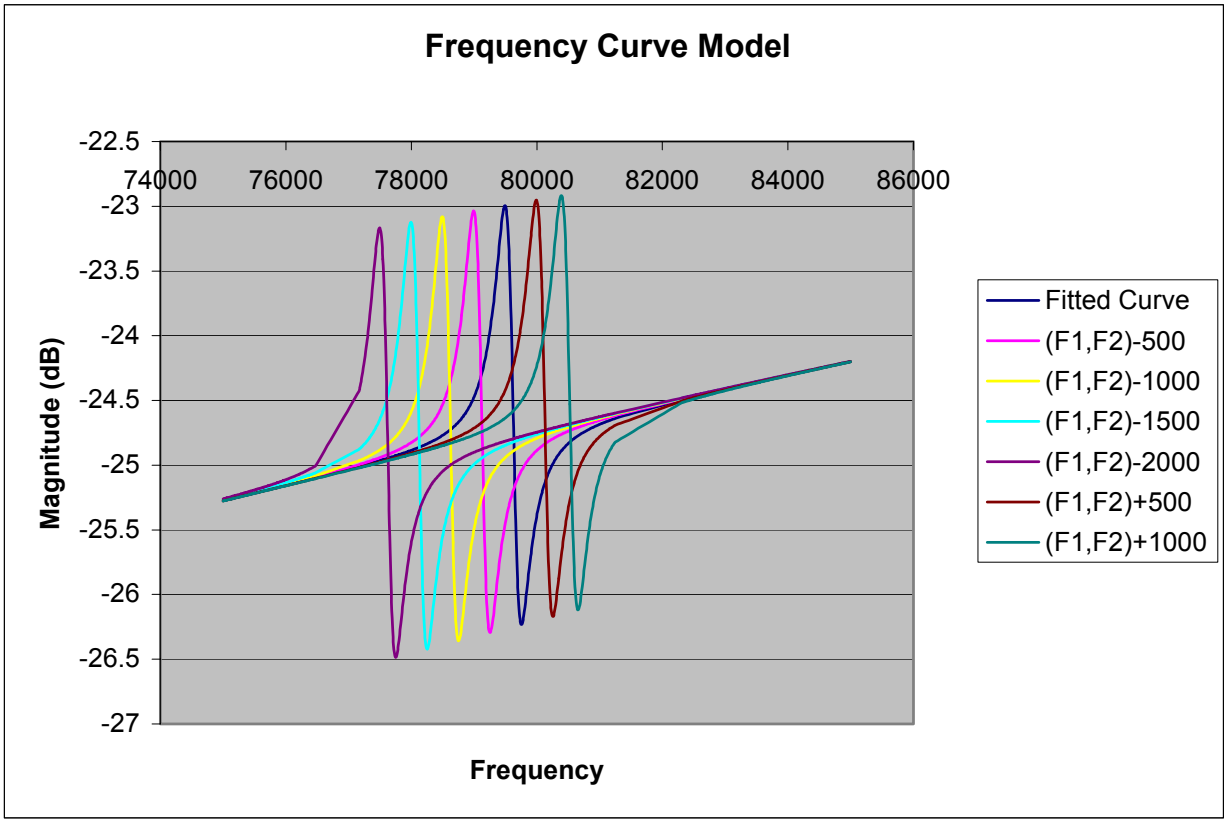

Figure 22: The Plot of the Empirical Data and Frequency Curve Fitted Model for Variation in Natural Frequency parameter

5.1.3 Variation in Damping Ratio Parameter

Further more, the frequency response model of the dynamic structure evaluate for the changing of the damping ratio parameter ξ as shown in the following figures.

The damping ratio is defined as:

$$\xi = \frac{R}{2LF_n} \qquad [5.1\text{-}1]$$

$$\xi = 2.313$$

The damping ratio is a parameter ξ , which is a dimensionless quantity that characterizes the frequency response of a second order ordinary differential equation. It is particularly important in the study of control theory. The behavior of the system depends on the relative values of the two fundamental parameters, the natural frequency, and the damping ratio (Smith, 1988).

The small value for damping ratio shows that the capacitance and inductance of the device is about 500 x the resistance, which confirms the value of resistance that we obtain in chapter 4 of this paper.

As the value the damping ratio increases, it cause the amplitude resonance to become smaller, and wider.

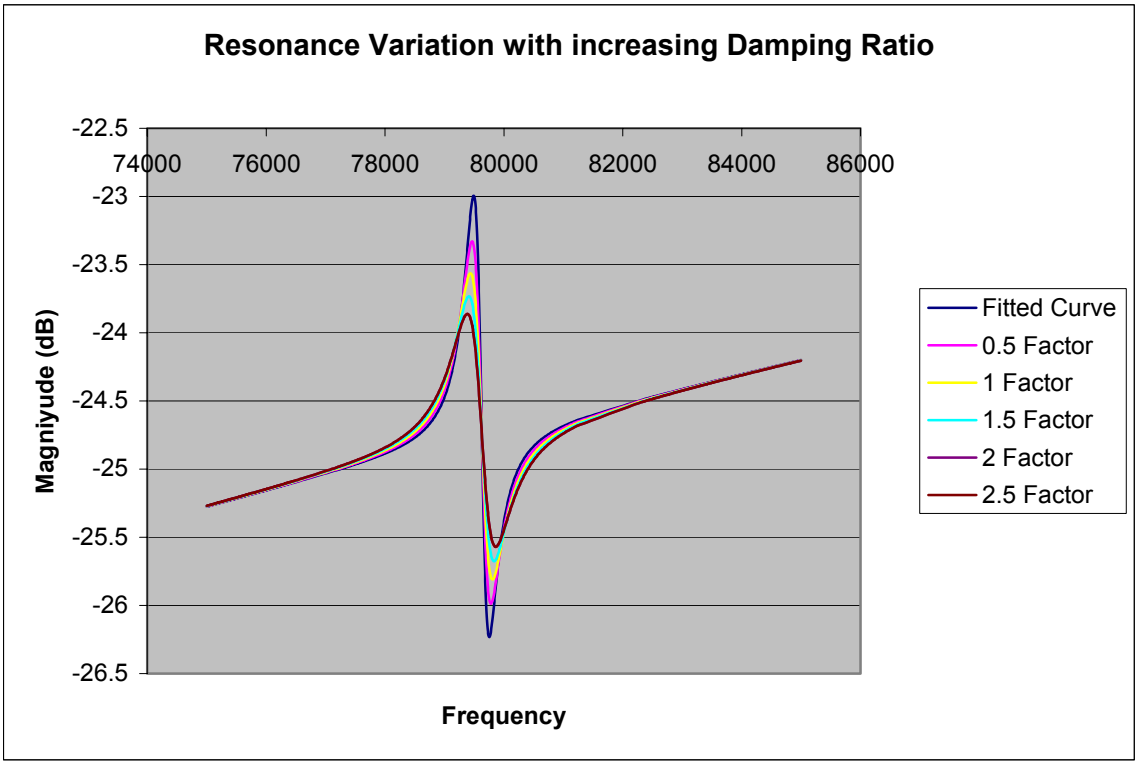

Figure 23: Illustrate the Effect of the Increasing Damping Ratio on the Resonance Characteristic with Curve Fitted Frequency Model

As the damping ratio increases, the amplitude resonance, grows smaller and wider.

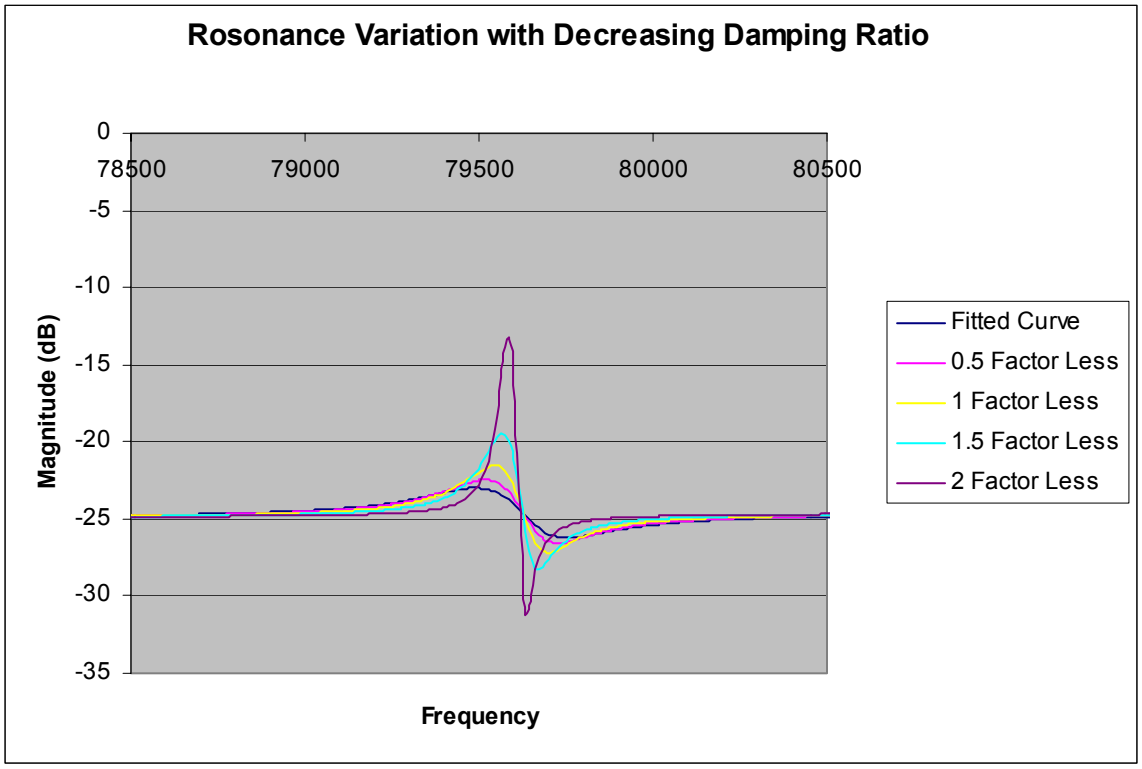

Figure 24: Illustrate the Effect of the Decreasing Damping Ratio on the Curve Fitted Frequency Model

As the damping ratio decreases, the resonance grows bigger and sharper. This behavior is consistent for all of the variations. The damping ratio has increases and deceases by factor $\pm 0.3, \pm 0.5, \pm 0.7, \pm 0.1, \pm 1.5, \pm 2$. The illustrated graphs were selected based on the clearly observable resolution of the results.

5.1.4 Variation in Cimage Parameter

The Cimage parameter is a factor that takes into account to match the 20 db increasing slope of bode plot of the system. The value for that in the best curve fitted model is 7.27e-07.

It observes that large Cimage parameter value as shown in the following graph causes the shift of the frequency curve fitted model upward, and small Cimage parameter causes the shift of the frequency curve fitted model downward.

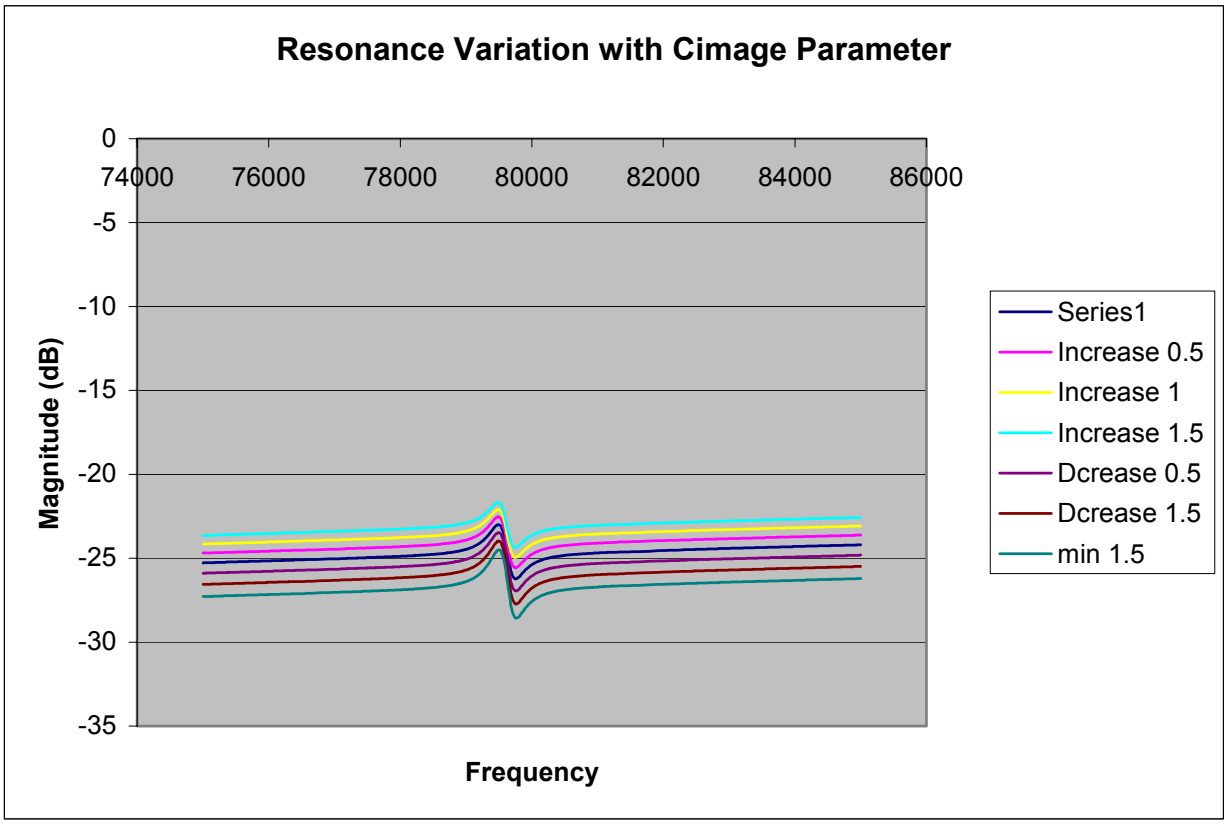

Figure 25: Illustrate the Effect of the Increasing Value of the Cimage on the Frequency Curve Fitted Model

5.2 Signature Recognition

The goal of pattern recognition is to classify objects into a number of classes. These objects are based on the application, such as signal waveforms, images or other measurement types. Algorithms or classifiers can be used for pattern recognition. This research effort focused on comparative studies of various techniques in the context of various applications.

By definition, piezoelectricity is the electricity (electric charge) generated in a material when a mechanical force is applied. A self-excited force pressure transducer is vibrated at its resonance frequency by applying an ac voltage to its piezoelectric layers. This section presents a technique for determining the condition of the pressure transducer. A completely broken sensor or disconnection in the line can both be identified easily due to lack of signal; however differentiating these failure modes can yield cost improvements. If only a small fracture occurs in the sensor, it still produces a signal with distortion, which can lead to false information and reliability issues (Park et al. 2006). Predicting degradation of the piezoelectric sensor by adjusting it during system downtime can yields substantial savings.

We present a technique to stimulate the piezoelectric element of the pressure transducer in the calibration frequency band, at conditions higher than the operating band. The frequency response characteristics captured across a shunt resistance, represent the variation of the sensor current due to capacitive impedance.

By monitoring changes in the shape and location of the resonance frequencies, via electrical simulation technique certain calibration information can be determined including the capacitance of the sensor.

The signature recognition is the process of verifying the desired identity by checking the signature against samples kept in a database. The result of this process is usually a number between 0 and 1, which represents a fit ratio (1 for match and 0 for mismatch). The threshold used for confirmation/rejection decision depends on the nature of the application (Liang et al. 1994). The signature verification system has major components.

The first step is data capture, which is the process of converting the signature into digital form or designing a desired hardware and firmware to capture the target data in a digital form. The second step is preprocessing of data to transform the data into a standard format. The third step is extraction of the desired feature. Feature extraction is the process of extracting key information from the digital representation of the signature; in this case the resonance characteristic is the key information. The next step is comparison process and is defined as extracted features are matched with target data stored in a database. Usually, the output is a fit ratio. Performance evaluation is the decision step typically made based on the fit value.

5.2.1 Design the Hardware for Signature Comparison

The purpose of this thesis is to explore the effectiveness of resonance base on the line field calibration from both hardware and software standpoints. Over thirty broken sensor test and data collect and analyzed. The completely broken transducers does not show resonance characteristic in the specified range, as shown by below graph. The sensor breakage changes the resonances of piezoelectric pressure transducer (Park et al. 2006).

The propose identification method is based on monitoring the resonance of the piezoelectric pressure transducer measured by electrical impedances.

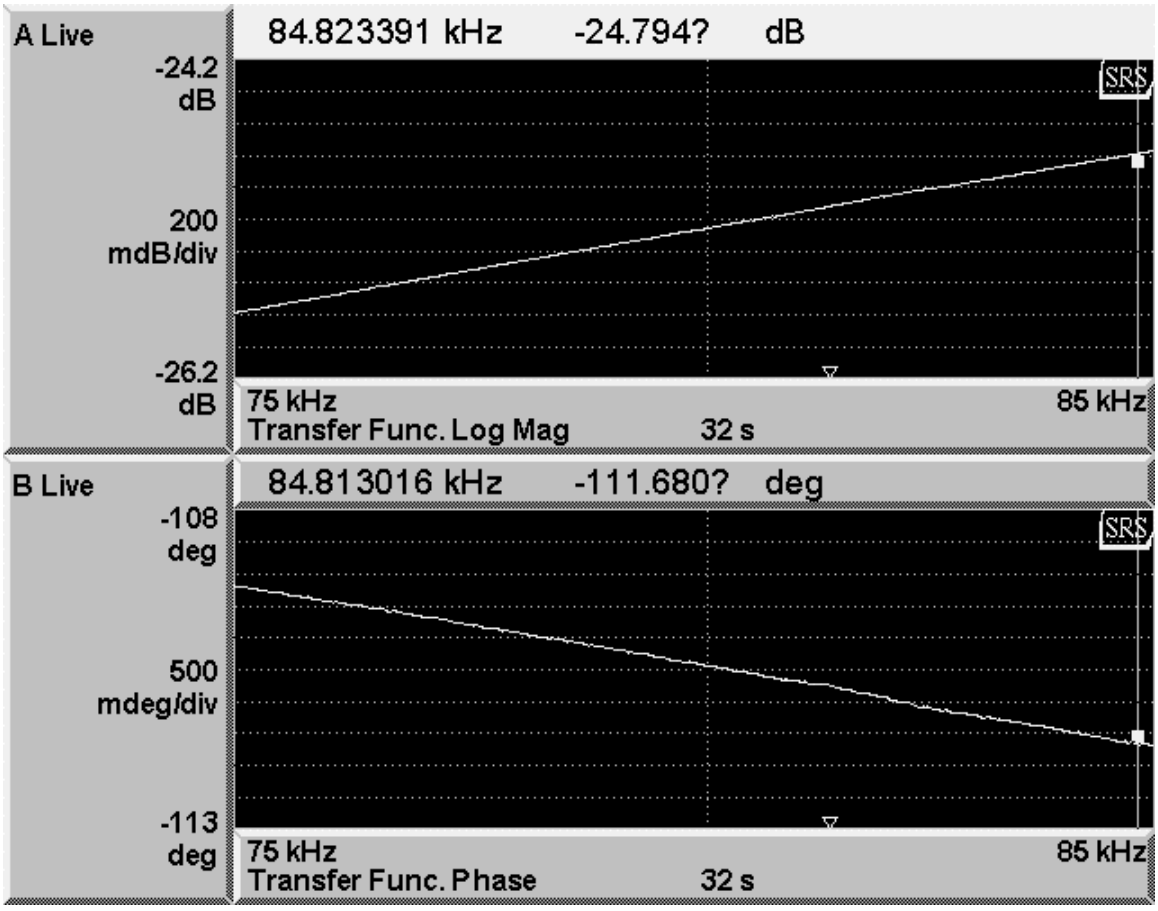

Figure 26: The Response of Completely Broken Sensor to Electrical Excitation

In a very few cases the characteristic is present with amplitude less than 75% reduction as shown in the following graph that capture, by electrical excitation of the broken sensor at desire frequency range. It leads us to conclude the absence of resonance characteristic or amplitude reduction at certain factor as damage in the sensor structure. The hardware generates the sine wave with desired amplitude of 2.8 V, and captures the response of the

sensor across shunt resistor. The voltage across shunt resistor is same as current response of the sensor, which goes through current amplifier for amplification. The sweep of frequency is control by the Field Programmable Gate Array (FPGA) on the circuit board.

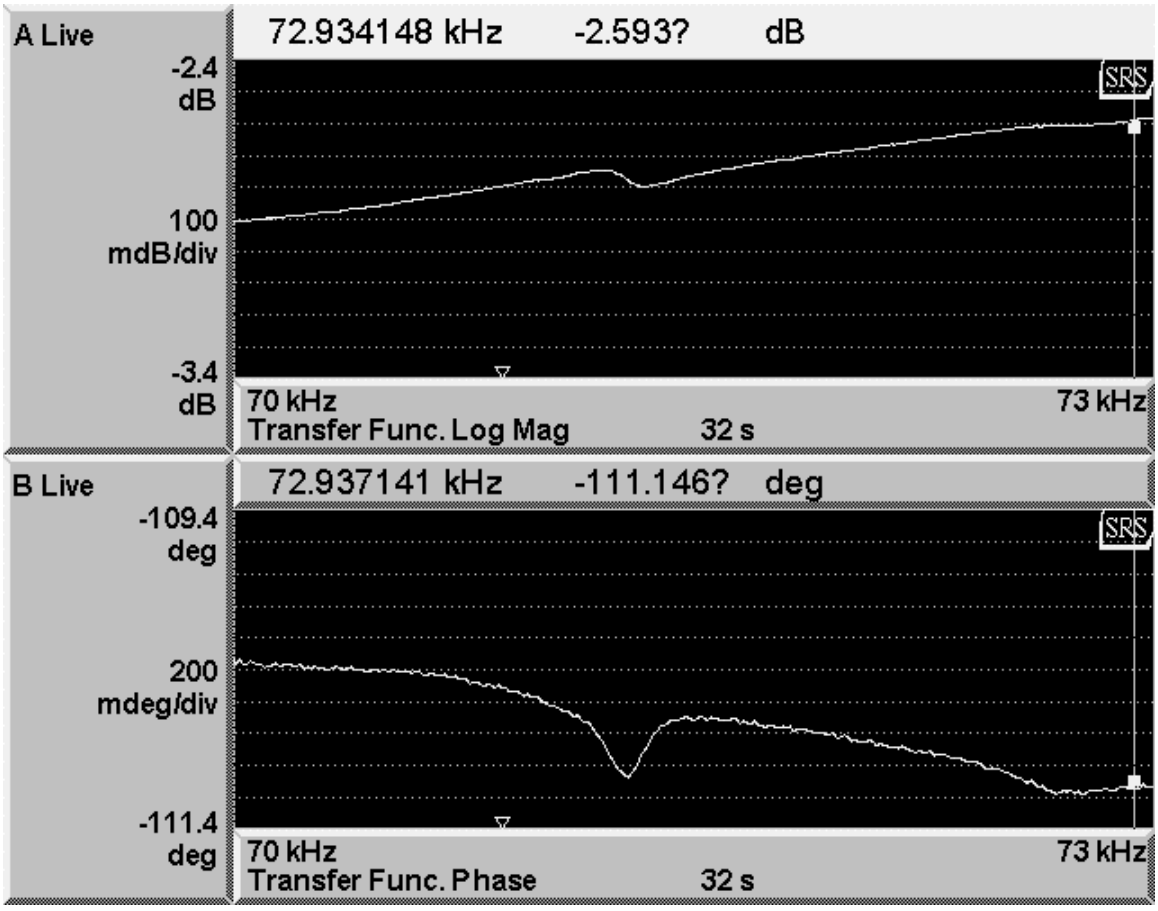

Figure 27: The Response of Completely Broken Sensor to Electrical Excitation with more than 75% Reduction in the Amplitude

FPGA is a semiconductor device that has programable logic components and programmable interconnects.

The controller performs FFT on the response signal and save two important pieces of information as magnitude and frequency in the specified location of memory.

5.2.2 Design the Firmware Algorithm for Signature Comparison

All of the healthy pressure transducers that we test for this research and experiments show a resonance frequency characteristic in ranges of 75 KHz-85 KHz. The sensor breakage changes the resonances of the piezoelectric pressure transducer. The new damage detection method, by monitoring the resonance characteristic of the piezoelectric pressure transducer, is a class of vibration based non-destructive evaluation. The design hardware sends the excitation signal to a sensor and captures two important pieces of information as magnitude and frequency of the response in the specified memory location. A data analyzer firmware is developed in this section. This tool analyses the sensor data gathered from the field by comparing it with the reference data. Reference data is the data that is captured by performing tests on healthy sensors. A consistent response pattern is recorded over the defined frequency range.

The analyzer evaluates the field-captured data with the reference patterns and detects/predicts the sensor is health. It performs multiple calculations on the waveform.

- Calculates the amplitude peaks and detects the amplitude shift.
- Calculates the frequency trends and detects abnormal frequencies.
- Predicts the sensor status by calculating its relative life.
- Shows user if the sensor has completely failed and needs replacement.

5.2.2.1 Inputs to the Tool

The tool expects the reference data and the field data in a comma separated values (CSV) format. It has a CSV parser built in that reads in this data and creates internal data arrays that will be use for analysis. The CSV file should contain two columns, the first column

for the frequency and the second column for the amplitude. No column header information is required.

The tool accepts the CSV file names as command line arguments. The order of the arguments is important; the first argument should be the reference data and the second should be the field data. Following is the command format:
>**Analyze** <RefData.csv> <Data.csv>
The internal buffer length is 1000 elements. If the CSV file contains more than 1000 rows, data is truncated.

The tool throws an error if it cannot find the input data files in the path it is running from. If the CSV files are saved at a different location than the tool itself, one should specify the full path with the name of the input files at the command line.
The tool does not perform any special checks to ensure the file integrity. It may crash if invalid files are input. The list of functions that the tool perform is described in the following sections.

5.2.2.2 Peak Detection (Amplitude Shift)

Once the parsing of data is complete, the tool performs a scan of the data to find the amplitude peaks (both upper and lower) on the reference data and saves the information. This saved information is later used to analyze the field data. The maximum and minimum amplitude is required for us to both validate weather the sensor is OK or not and to predict its state.

It has been observed historically that when the sensors start deteriorating the response amplitude drops. When the drop is around Reference Amplitude / 7 it implies that the sensor has completely gone bad.

The peak detection logic analyses the amplitudes to see to what level the amplitude fell. If it is A/7 then the sensor is declared as bad, otherwise it reports the sensor status over a scan of A/1 to A/7.

5.2.2.3 Frequency Shift

The tool analyzes the frequency information to see if the amplitude varies per the desired frequency levels. It does this by comparing the amplitude values against the reference frequencies. It is possible that the response is just a straight line (no amplitude variation across the frequency range) indicating the either the senor data is invalid or the sensor is bad.

It is also possible that the there is a slight frequency shift in the field data as compared to the reference data. The firmware finds the differences and reports on the console.

5.2.2.4 Software Design

The Analyser class:

```
class cAnalyzer
{
private:
        //Data variables.
        double mFreq[MAX_DATA_SIZE]; //Buffer to store frequency data
        double mAmpl[MAX_DATA_SIZE];          //Buffer to store amplitude data
        double mRefFreq[MAX_DATA_SIZE]; //Buffer to store reference frequency data
        double mRefAmpl[MAX_DATA_SIZE]; //Buffer to store reference amplitude
data

        //Counters
        int mDataCount;
        int mRefDataCount;

        //Max Min offsets
        //We use these variables to save the min/max offsets
        //to be retreived for displaying.
        int mMaxOffset;
        int mMinOffset;
```

```
        int mRefMaxOffset;
        int mRefMinOffset;
public:
        //Constructor
        cComparer();

        //Destructor
        ~cComparer();

        //Load the data file
        int LoadFile(char *FileName);

        //Load the reference file
        int LoadRefFile(char *FileName);

        //Calculate Min Max on data
        int CalculateMinMax();
        int CalculateRefMinMax();

        //Check if data is within 1% of reference;
        int ValidateData();

        //Find the amount of shift
        int FindPercentAmplShift();
        int FindPercentFreqShift();

        //Display methods
        double GetMaxAmpl()             {return mAmpl[mMaxOffset-1];}
        double GetMinAmpl()             {return mAmpl[mMinOffset-1];}
        double GetMaxRefAmpl()    {return mAmpl[mRefMaxOffset-1];}
        double GetMinRefAmpl()    {return mAmpl[mRefMinOffset-1];}
};
```

Private members:

The buffers used to store the data are defined as fixed arrays of size 1000.

Public members/Methods:

We have members that perform the file load operation and a set of functions that performs specific analysis on the data.

There are some helper methods that are used to display analyzed data on the console.

A helper class has been created to parse the CSV file.

```
class cCSVReader
{
private:
        ifstream mFile;          //The file handle
        string mData;         //The Data
        string::size_type mPos;          //Current Position in the data buffer
        void SkipSpaces(void);

public:
        //Constructor
        cCSVReader(char *Filename);
        //Destructor
        ~cCSVReader();
        //Function to read a single line from file
        int ReadNextLine();
        //Function to check if there is any data in the buffer
        bool IsDataEmpty(){return (mData == "");}

        //operator overloads to read the comma separated values.

        //Read an integer value
        cCSVReader & operator >> (int &Integer);
        //Read an long value
        cCSVReader & operator >>(long & Long);
        //Read a double value
        cCSVReader & operator >> (double &Double);
        //Read a string
        cCSVReader & operator >> (string &String);
};
```

5.3 Correlation of the Model Parameters with Sensitivity Variation

The sensor is excited with a sinusoidal signal with a frequency analyzer from 100 Hz to 100 KHz, with an excitation voltage of 2.8 V pp. The output voltage is observed by a shunt resistance of 20 Ω. 14 different sensors with the sensitivity deviation of Δ2 were tested to investigate correlation. After each set of data was collected from the frequency analyzer, they were converted to readable format. The least square method is used in these experiments for curve fitting of each set of data, and for parameter estimation. The Excel software implemented the optimization to capture the best parameters for each sensor. The results for the correlation of each parameter and sensitivity are discussed in this section.

Minitab Statistical Software is used in this project as a tool to analyze data and perform statistical analyses. Its power and ease of use make it the leading package use for quality improvement and statistics education worldwide. Minitab provides an intuitive, and user-friendly menu that guide toward a correct statistical analysis.

One of the statistical techniques, which can show whether and how strongly pairs of variables are related, is correlation. There are several different correlation techniques. The most common type called the Pearson or product-moment correlation. This type is useful when one wants to look at the relationship between two variables while removing the effect of one or two other variables. The main result of a correlation is called the correlation coefficient, which ranges from -1.0 to +1.0. If the correlation coefficient is close to 0, it means there is no relationship between the variables. Positive correlation coefficient means that as one variable gets larger, the other gets larger, and negative correlation coefficient means that as one gets larger, the other gets smaller. The Pearson correlation technique works best for the statistical analysis of this project because we are investigating the linear relationship between sensitivity and model parameters. The

Pearson correlation formula has many forms. One of the most common forms is shown below:

$$r = \frac{\sum AB - \frac{\sum A \sum B}{N}}{\sqrt{\left(\sum A^2 - \frac{\left(\sum A\right)^2}{N}\right)\left(\sum B^2 - \frac{(B)^2}{N}\right)}} \qquad [5.3\text{-}1]$$

The correlation coefficient is r, and N is the number of samples. A and B are variables measured on the same object. Marginal plot is used to show the relationship between sensitivity and model parameters. This plot is a scatterplot with histograms, boxplot, or dot plot in the margins of the x-axes and y-axes. The statistical analysis performed in this section uses marginalplots with a histograms option. It needs two numeric or date/ columns of equal length. The first graph is the relationship between sensitivity and damping parameter.

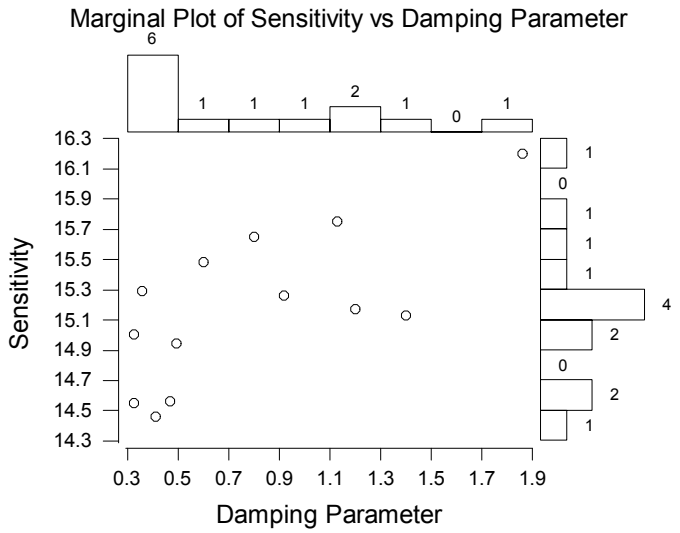

Figure 28: Marginal Plot of Sensitivity vs. Damping Parameter

The scatter plot shows a possible positive correlation between sensitivity and damping parameter; that is damping parameter increases as sensitivity increase. These results leads to the conclusion that as sensitivity increases, the sharper response in resonance characteristic. The correlation coefficient calculated for this relationship has a value of 0.707, which confirms this relationship. The marginal distributions have clusters of points about 15.3 for sensitivity, and 0.3 for damping parameter. These results are obtained from the histogram.

The relation between the A parameter and model parameter follow the same pattern as damping parameter, since both control the magnitude at a natural frequency.

The second plot represents the relationship between sensitivity and natural frequency. The correlation coefficient of 0.378 is obtained from correlation calculation.

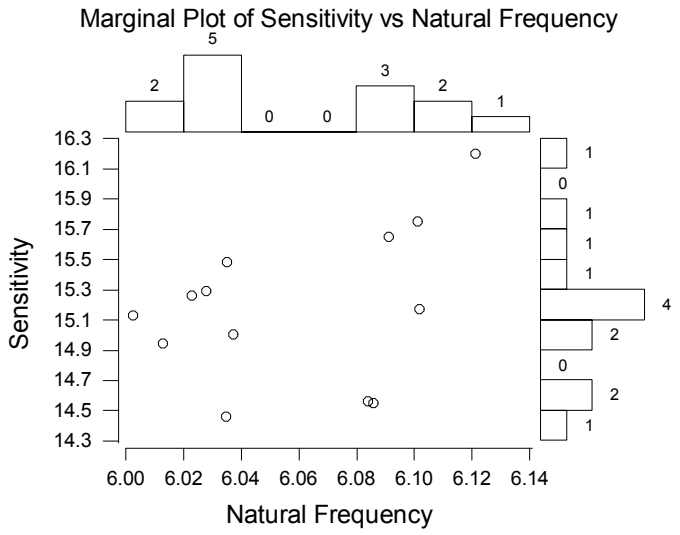

Figure 29: Marginal Plot of Sensitivity vs. Natural Frequency Parameter

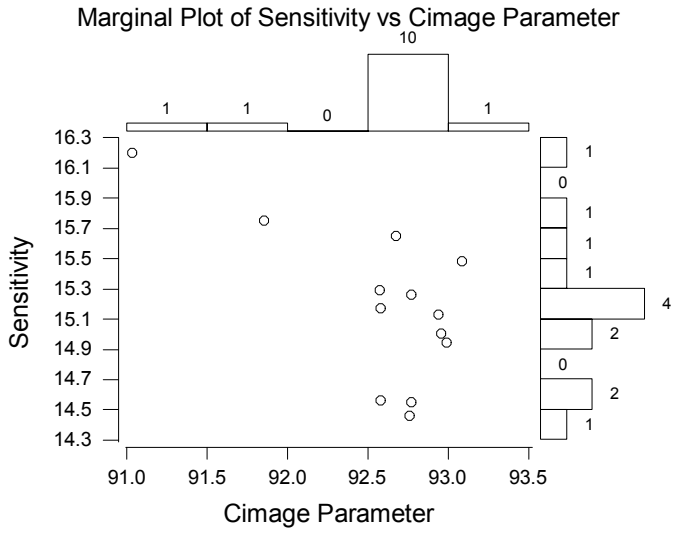

Figure 30: Marginal Plot of Sensitivity vs. C image Parameter

The scatter plots show a possible negative correlation between sensitivity and the

Cimage parameter. It is observed from the analysis explained in section 5.1.4 that a large Cimage parameter value causes an upward shift of the frequency curve fitted model, and small Cimage parameter causes the shift of the frequency curve fitted model downward. These results can lead to a conclusion that as sensitivity decreases the resonance characteristic moves upward. The correlation calculation reveals the value of –0.653, which confirms the inverse relationship.

One great way to conclude the absolute relationship between each of these parameters and sensitivity is to investigate this analysis with a larger number of sensors along with larger deviation in sensitivity. In order to completely perform prognosis, the analysis must be followed for each sensor and their conditions over time. These issues are currently under investigation by the author.

5.4 Detection of Sensitivity Change Based on Impedance Monitoring

The sensor field calibration is a critical component in confirming the proper functioning and reliability of data. The process with a large number of active sensors installed in the structure is very cost effective. This section studies the relationship between the impedance value and the sensitivity of the sensor to track the degradation of the electrical/mechanical properties of the pressure transducer.

It is very rare that the sensitivity of the piezoelectric sensor changes and capacitance remain the same. On the other hand, the slope of the impedance plot is proportional to the capacitance by the following relationship:

$$\frac{I_{sensor}}{V_{in}} = \frac{V_{sensor} / Z_{sensor}}{V_{in}}; Z_{sensor} = 1/\ jwc; I_{sensor} = jwcV_{sensor} \qquad [5.4\text{-}1]$$

It is desired to investigate the relationship of impedance value at a certain frequency for sensors with different sensitivities. Since the magnitude of the current coming from sensor is very small about 120 *mA*, an amplifier circuit with a gain of 20 designed and built to observe the slope value better. Typically, these measurements are made using a frequency analyzer such as SRS. The impedance at each frequency is proportional to capacitance of the piezoelectric pressure transducer, and the sensitivity of the device is related to the capacitance. The frequency analyzer measures the magnitude of electrical impedance *Z*, which is a combination of both resistive, *R* and reactive characteristic, X, and can be calculated by following formula:

$$Z = \sqrt{R^2 + X^2} \qquad [5.4\text{-}2]$$

The reason to select FTT to measure impedance is that it can be implemented on a computer chip. The electrical impedance of the sensor is equal to the excitation voltage divided by the current through the sensor. The impedance generated is the (*Vout*) across shunt resistor over the excitation voltage (*Vin*). The shunt resistor is connected in a series with a sensor. The shunt resistor was choosen to be as small as possible to have voltage drop across resistor proportional to current generate by sensor. The approximate impedance Z is

$$Z = \frac{V_{in}}{I} = \frac{V_{out} R_{shunt}}{V_{in}} \qquad [5.4\text{-}3]$$

The current gain amplifier is designed to increase the gain by factor of 20. The gain may be calculated by the following equation:

$$G = \frac{R_2}{R_1} = \frac{200}{10} k = 20 \qquad [5.4\text{-}4]$$

The circuit to calculate the impedance of a sensor, and its connection to current amplifier is shown.

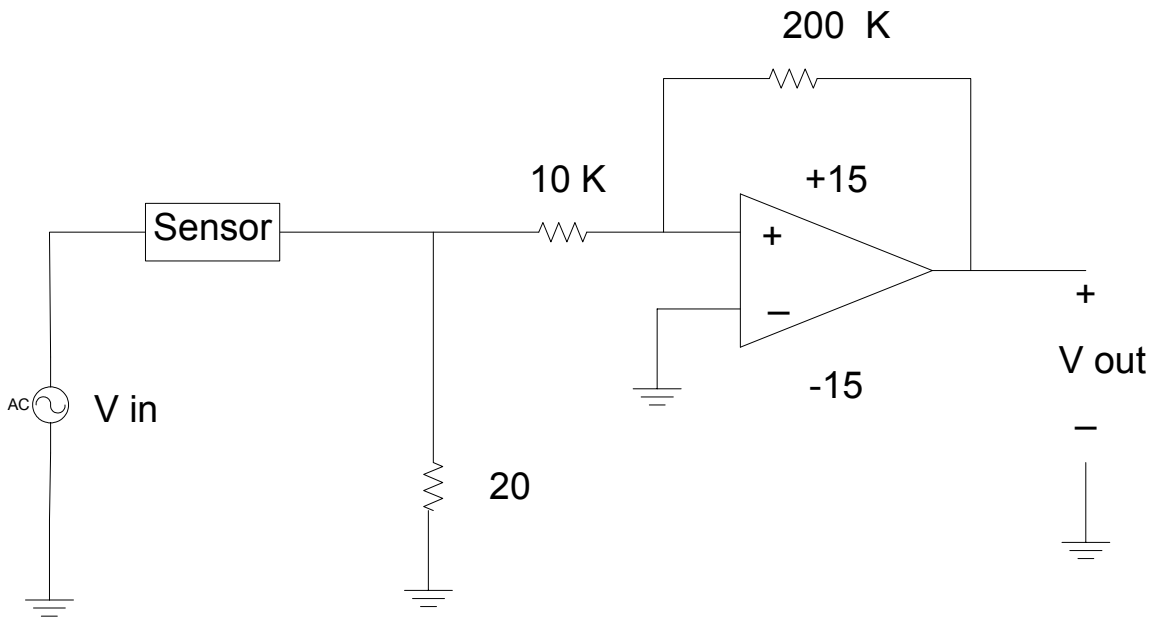

Figure 31: Impedance Measurement Circuit with Current Amplifier

In order to investigate the relationship between sensitivity and impedance, a total of 14 sensors with sensitivity variations of Δ2 is tested. The value of the impedance at a unique frequency is (62000 Hz) is recorded. The analysis shows a possible negative correlation between impedance magnitude and sensitivity.

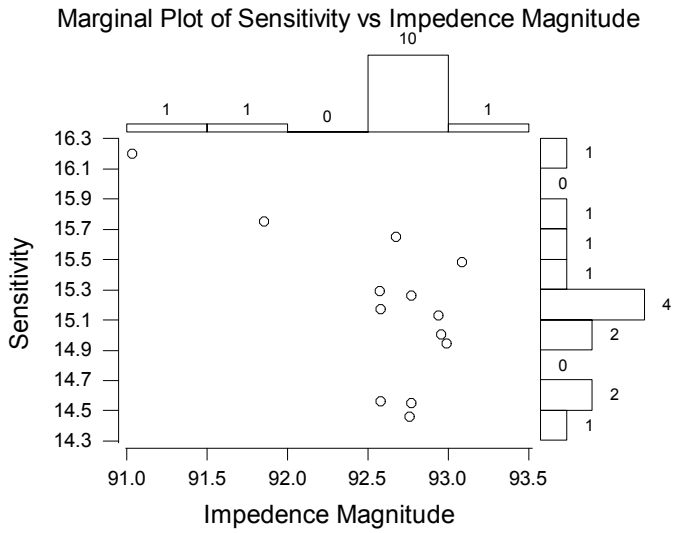

Figure 32: Marginal Plot of Sensitivity vs. Impedance Magnitude

The analysis was performed on a set of data and correlation coefficient of –0.602 confirms the above possibility. Theses analysis of larger numbers of sensors along with larger deviations in sensitivity is under investigation by the author. The magnitude of impedance measures for each sensor contains an R component, and an X imaginary component of impedance. The R component is generally employed for structural health monitoring, because R is more reactive to damage or changes in structural integrity. The imaginary part of impedance changes is due to capacitance of sensor or cable. The capacitance value changes are due to temperature or other disturbances in the environments. All these factors need to be considered in the design a method based on impedance monitoring.

Other analyzers may use an impedance measurement health monitoring technique that measures the real part and imaginary part of impedance separately. Such an analyzer lacks characteristics desired for the impedance health monitoring like a frequency sweep mode. An FFT analyzer, such as the one used in these experiments, is more common and

less expensive than an impedance analyzer. It also has the benefit of being implemented on a computer chip, which is more reflective of real life applications.

CHAPTER VI

CONCLUSIONS

A model for a desired pressure transducer developed by system identification techniques and parameter estimation. The system model was developed based on time domain and frequency domain data. From frequency domain data, the Bode plot of the system captured, and Least squares method and regression analysis heavily performed to estimate parameter and develop a frequency curve fitted model. From the frequency curve fitted model, the differential equation models were developed.

The comparisons between the time domain model and differential equation model were performed by applying the same step response in time domain to the differential equation model. The results for two models were discussed.

The extension of this work to test the model with background noises to simulate a real environment, which guarantees the excitation of the sensor in the field, is currently being investigated by the author, and will be explored in a future paper. The circuit board to stimulate natural frequencies of the pressure transducer on the field to collect statistical data is currently under development by the author.

These studies can greatly help the engineering community to model sensor behavior to predict its characteristics and natural frequency response. It also contributes greatly in developing the circuit to be tested on the field for collecting statistical data of the pressure transducer's working conditions based on the shape and location of the resonance frequency response of the sensor. More over, the new idea of measuring the capacitance of the pressure transducer based on the gain of the system was investigated during this work.

The relationship between resonance frequency characteristics and model parameters was investigated, and a correlation coefficient was calculated for each parameter. The analysis was performed on 14 healthy sensors with sensitivity deviations of $\Delta 2$ to investigate the correlation of sensitivity and each model's parameters. In order to completely perform prognosis, the analysis needs to be followed for each sensor and its conditions over time. The investigation will be continued by the author with larger number of sensors along with larger deviations in sensitivity to conclude the absolute relationship between each of these parameters and degrees of sensitivity.

LITERATURE CITIED

[1] Cady, Walter G., "Piezoelectricity," Dover Publications, New York, Copyright 1964.

[2] Wilson, Jon S., "Sensor technology handbook," Elsevier Inc., Burlington, Copyright 2005.

[3] Kirk, Donald E., "Optimal Control Theory An Introduction," Dover Publications, Mineola, New York, Copyright 1998.

[4] Raol, J.R, Girija, G., Singh, J., "Modeling and Parameter Estimation of Dynamic System," The Institution of Electrical Engineers, London, United Kingdom, Copyright 2004.

[5] Meirovitch, L., "Element of Vibration Analysis," The McGraw-Hill Companies Inc., New York, Copyright 1986.

[6] Frequency Response Analysis and Design
http://www.engin.umich.edu/group/ctm/freq/freq.html

[7] Ljung, L., "System Identification: Theory for the user," Prentice-Hall, Inc., Englewood Cliffs, New Jersey, Copyright 1987.

[8] Biot, Maurice A., Karman, T., "Mathematical Methods in Engineering: An Introduction to the mathematical Treatment of Engineering," The McGraw-Hill Companies Inc., New York, Copyright 1940.

[9] Smith, J., "Vibration of Structures: Applications in Civil Engineering Design," Chapman and Hall., New York. Copyright 1988.

[10] Park, Farrar, Rutherford, Robertson, "Piezoelectric Active Sensor Self-Diagnostics using Electrical Admittance Measurements," Journal of Vibration and Acoustics, 2006. Page(s):469 - 476 vol.128

[11] Saint-Pierre, N., Jayet, Y., Perrissin-Fabert, I., and Baboux, J. C., 1996, "The Influence of Bonding Defects on the Electric Impedance of Piezoelectric Embedded Element," J. Phys. D, 29, pp.2976-2982.

[12] Simmers, G. E., Hodgkins, J., Mascarenas, D., Park, G., and Sohn, H.,2004, "Improved Piezoelectric Self-Sensing Actuation,"J. Intell. Mater. Syst. Struct., 15, pp. 941-953

[13] Atherton, W. J., Flanagan, P. M., "A Self Diagnostic System For Piezoelectric Sensors," American Institude of Aeronautics and Astronautics, Inc., 1989. Cleveland State University Cleveland, OH

[14] Bronson, G. J., "C++ for Engineers and Scientists," Brooks/Cole Publishing Company, Pacific Grove, California, Copyright 1999.

[15] Liang, C., Sun, F.P. and Rogers, C.A. (1994) "Coupled Electromechanical Analysis Of Adaptive Material Systems-Determination of the Actuator Power Consumption and System Energy Transfer," Journal of Intelligent Material Systems and Structures, 5, 12-20

[16] Doebling, S.W., Farrar, C.R., and Prime, M.B. (1998). "A summery Review of Vibration-Based Damage Identification Methods," The Shock and Vibration Digest Journal, V.30, 91-105

[17] Lifshitz, J. M., Rotem, A. 1969 "Delamination of Reinforcement Unibonding of Composites by a Vibration Technique," Journal of Composite Materials, Vol. 3, 412-423.

[18] Adams, R. D., Cawley, P., Pye, C.J. and Stone B. J. 1978 "A Vibration Technique for Non-Destructively Assessing the integrity of Structures," Journal of Mechanical Engineering Science, 20 93-100.

[19] Farrar, C. R., Baker, W. E., Bell, T. M., Cone, K. M., Darling, T. W., Duffey, T. A., Eklund, A. and Migliori, A. 1994 "Dynamic Charactrization and Damage Detection in the I-40 Bridge Over the Rio Grande," Los Alamos National Laboratory Report LA-12767-MS.

[20] Staszewski, W.J. 1999 “Structure and mechanical Damage Detection Using Wavelets,” Shock and Vibration Digest, Vol. 12-27

[21] Spillman, W, Huston, D., Fuhr, P., and Lord, J., 1993. “Neural Network Damage Detection in a Bridge Element,” SPIE Smart Sensing, Processing, and Instrumentation, V. 1918, pp. 288-295.

[22] Crawley, E. F. AND Anderson, E. H. 1990 “Detailed Models of Piezoceramic Actuation of Beams,” Journal of Intelligent Material Systems and Structures, Vol. 1, 4-25.

[23] Worden, K., Ball, A., and Tomlinson, G. 1993. “Neural Networks for Fault Location,” Proceeding of the 11th International Modal Analysis Conference, pp. 47-54.

[24] Pearson Correlation

http://www.childrens-mercy.org/stats/definitions/correlation.htm